Recent Progress on Titanium Dioxide Nanomaterials for Photocatalytic Applications

Maryline Nasr, Cynthia Eid, Roland Habchi, Philippe Miele, Mikhael Bechelany

▶ **To cite this version:**

Maryline Nasr, Cynthia Eid, Roland Habchi, Philippe Miele, Mikhael Bechelany. Recent Progress on Titanium Dioxide Nanomaterials for Photocatalytic Applications. ChemSusChem, 2018, 11 (18), pp.3023 - 3047. 10.1002/cssc.201800874 . hal-01895429

HAL Id: hal-01895429
https://hal.umontpellier.fr/hal-01895429v1

Submitted on 4 Jun 2021

HAL is a multi-disciplinary open access archive for the deposit and dissemination of scientific research documents, whether they are published or not. The documents may come from teaching and research institutions in France or abroad, or from public or private research centers.

L'archive ouverte pluridisciplinaire **HAL**, est destinée au dépôt et à la diffusion de documents scientifiques de niveau recherche, publiés ou non, émanant des établissements d'enseignement et de recherche français ou étrangers, des laboratoires publics ou privés.

Recent Progress on TiO_2 Nanomaterials For Photocatalytic Applications

Maryline Nasr,[1,2] Cynthia Eid,[2] Roland Habchi,[2] Philippe Miele[1,3] and Mikhael Bechelany*[1]

[1]Institut Européen des Membranes IEM, UMR-5635, Université de Montpellier, ENSCM, CNRS, Place Eugène Bataillon, F-34095 Montpellier Cedex 5, France

[2]EC2M, Faculty of Sciences 2, campus Pierre Gemayel, Fanar, Lebanese University, 90656 Lebanon

[3]Institut Universitaire de France (IUF), MESRI, 1 rue Descartes, 75231 Paris cedex 05, France

* Corresponding author: mikhael.bechelany@umontpellier.fr

Phone: +33467149167, Fax: +33467149119

Table of Contents

1. Abstract

Environmental and energy problems have drawn much attention due to the rapid population growth and the accelerated economic development. For instance, photocatalysis, “a green technology”, plays an important role in solar energy conversion owing to its potential to solve energy and environmental problems. Recently, many efforts have been devoted to improve the visible-light photocatalytic activity using titanium dioxide as photocatalyst due to its wide range of applications in energy and environment fields. However, the fast charge recombination and the absorption edge in the UV range limits the photocatalytic efficiency of TiO_2 under visible-light irradiation. Many investigations have been carried out in order to overcome the limitations of TiO_2 and therefore enhance its photocatalytic activity under visible light. The present literature review focuses on different strategies used to promote the separation efficiency of the electron-hole pairs and to shift the absorption edge of TiO_2 to the visible region. Current synthesis techniques used to elaborate several nanostructures of TiO_2 based material, recent progress in enhancing visible photocatalytic activity and the different photocatalysis applications will be discussed. Based on the studies reported in the literature, we believe that this review will help in the development of new strategies to further improve the visible light photocatalytic performance of TiO_2 based materials.

2. Introduction

In recent years, there has been great concern over many serious environmental and energy problems we are facing all over the world [1]. One of them concerns the safety of water, our most important natural resource [2]. The need for clean water put more stress on the removal of organic pollutants, and toxic heavy metal ions from water sources [3,4]. Several techniques are already used for the treatment of water such as absorption with or without chemical reaction [5-7], adsorption [8], condensation [9], biological degradation and

photocatalysis [10]. The adsorption techniques on highly porous materials have the disadvantage of transferring the pollutants to another phase without destroying them. Thus, their destruction requires the subsequent use of filters [11], while the ideal solution should be applicable to all types of pollutants and should not consume energy or emit environmentally harmful by-products [12]. Moreover, the increasing of CO_2 concentration in the atmosphere due to the high consumption of fossil fuels causes an energy crisis and leads to global warming. Recently, research attention has been devoted to reduce CO_2 emission by converting solar energy into chemical energy[13]. Therefore new effective and low cost technologies are required with the ability to solve energy and environmental pollution problems[14,15]. Photocatalysis has appeared as an innovative and promising technology with the advantage of converting the solar energy into chemical energy[16]. This technique has a wide range of applications such as photodegradation of pollutant and heavy metals, water disinfection, hydrogen generation, carbon dioxide photoreduction, photoelectric sensing and photodynamic therapy[17-22]. Figure 1 describes the principle of a semiconductor photocatalysis. The absorption of a photon by the semiconductor ($h\nu \geq E_g$) will cause the excitation of an electron from its valence band to its conduction band, creating a positively charged hole (h^+) in the valence band. The electron-hole pairs can migrate separately to the surface of the semiconductor and participate in the redox reactions in order to degrade or to reduce the adsorbed molecules (Equation 1 to 4) [16,23].

$$SC + h\nu \rightarrow h^+ + e^- \qquad \text{(Equation 1)}$$

$$H_2O + h^+_{(\text{valence band})} \rightarrow HO^\bullet + H^+ \qquad \text{(Equation 2)}$$

$$h^+_{(\text{valence band})} + \text{pollutant} \rightarrow \text{pollutant}^+ \qquad \text{(Equation 3)}$$

$$HO^\bullet + \text{pollutant} \rightarrow H_2O + CO_2 \qquad \text{(Equation 4)}$$

$$h^+ + e^- \rightarrow \text{heat} \qquad \text{(Equation 5)}$$

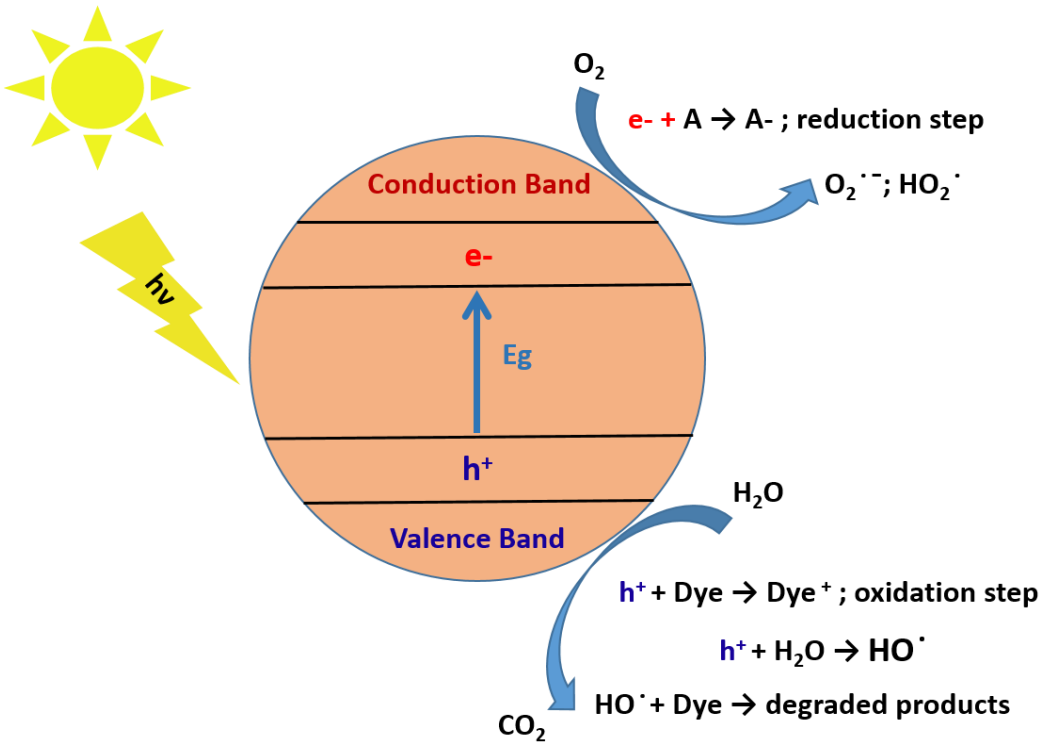

Figure 1: Schematic of a semiconductor photocatalysis.

In 1972, Fujishima and Honda [24] observed that under UV irradiation, the use of a TiO_2 electrode in an electrochemical cell lead to water dissociation, even without imposing an external voltage. This experiment demonstrates another property of TiO_2: its photocatalytic activity, thereby opening up a new field of application [25]. Till now, titanium dioxide is the most photoactive material [26] due to its oxidizing ability, chemical stability and low cost [27,28]. Anatase, rutile and brookite are the main crystalline phases of TiO_2. The three crystalline phases are all made up of an octahedron of oxygen atoms around a titanium atom (TiO_6 octahedras) but with a different organization depending on the kind of phase (Figure 2). The rutile is the most abundant form and crystallizes in the quadratic Bravais network. The rutile is formed of octahedras of oxygen atoms connected regularly in the direction [001]. The atoms are well organized in each face and thus contribute to the stability of the rutile phase. The anatase as well has a tetrahedral structure (also called quadratic) in the Bravais network. On the other hand, the anatase consists of irregular octahedras of oxygen atoms octahedral giving it an elongated structure. The brookite has an orthorhombic structure in which the octahedras of oxygen atoms are organized regularly (Figure 2) [29,30]. According to

previous studies, anatase TiO_2 has demonstrated a greater photocatalytic activity compared to other crystalline phases of TiO_2 [31]. However, till now TiO_2 has not yet reached the expected photocatalytic activity due to several limitations including the fast electron-hole pair recombination [32]. In addition, TiO_2 has a large band gap (Eg > 3.2 eV), and it can only be excited by ultraviolet light with a wavelength below 388 nm (equivalent to less than 7% of solar light) [33,34]. To overcome these limitations, several strategies have been investigated to improve the visible-light absorbance and increase the charge carriers life time of TiO_2-based photocatalyst [35,36]. Many review papers have been published to study the photocatalytic activity of TiO_2. Some of them focused on the photocatalytic process, reaction mechanisms and photocatalytic applications [17,37]. Other reviews focused on different TiO_2 nanostructures and preparation methods [38,39]. Some reviews investigated the effect of the photocatalysis operational parameters and the modification of TiO_2 properties[40-42]. To the best of the author's knowledge, none of these reviews (especially for the last two years) focused on all the above studies at the same time. Therefore, we believe that a new and comprehensive review of TiO_2 photocatalysis is needed in order to face all the limitations mentioned above and to further improve the visible photocatalysis of TiO_2.This review article will present the recent progress achieved in the TiO_2 nanomaterials for photocatalytic applications, under visible light. Firstly, we will define the most common synthesis techniques used to elaborate 0D, 1D and 2D nanostructures of TiO_2 nanomaterials. In order to achieve higher efficiency in photocatalysis, we will briefly describe the photocatalysis operating parameters and the different strategies used to tune TiO_2 photocatalyst properties including metal doping, surface modification with metal elements, modification with non-metal elements, coupling with other semiconductors and design of multiple components. We will also discuss the implication of TiO_2 in the various photocatalysis applications such as pollutant and heavy metals photodegradation, bacterial removal, hydrogen production, carbon dioxide photoreduction, photoelectric sensing and photodynamic therapy. Lastly, we will summarize the latest achievements of TiO_2 as a photocatalyst in large scale applications.

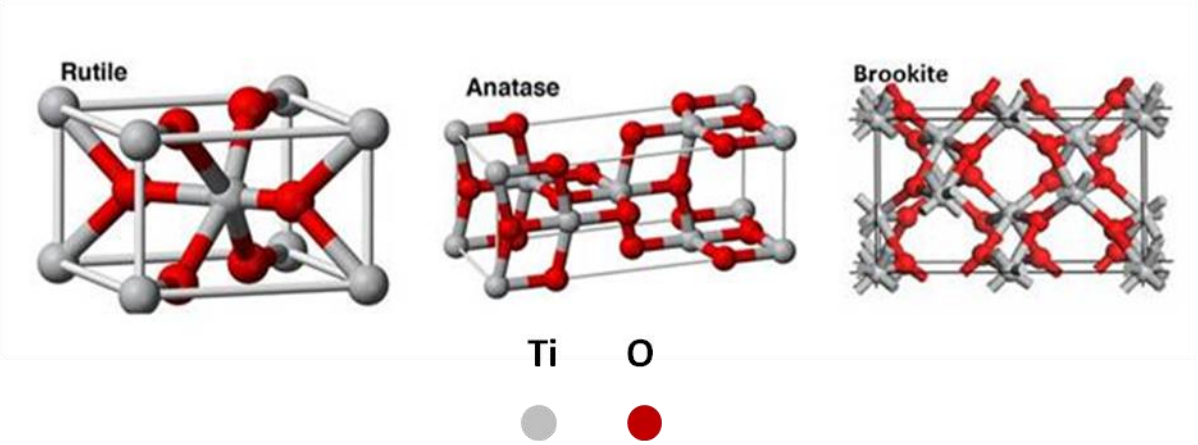

Figure 2: Crystalline phases of TiO_2 [43].

3. Synthesis techniques of multi-dimensional TiO_2 nanostructures

Previous studies showed that different morphologies (0D, 1D and 2D) of a photocatalyst may result in different photocatalytic properties [44]. This diversity can be achieved by a wide variety of titanium dioxide synthesizing methods [45]. The size, the morphology and the composition of titanium dioxide can be controlled by different parameters, such as titanium precursor concentration, pH, temperature, duration of treatment and the used chemical species [46,47]. The following section will focus on the most common synthesis techniques used to elaborate different nanostructures (0D, 1D and 2D) of TiO_2 materials with different sizes and morphologies including solvothermal, electro-deposition, electrospinning, hydrothermal, electrochemical anodization, template assisted method, sol-gel, spin coating, dip coating, chemical vapor deposition and atomic layer deposition.

3.1. Synthesis techniques of 0D TiO_2 nanostructures

0D nanostructures concern those with spherical shapes such as nanoparticles. These spherical particles have a large specific surface area which gives them a strong interest for photocatalytic applications, since the photoreactions occur on the surface of the photocatalyst. Several synthesis techniques were used to elaborate TiO_2 nanoparticles such as solvothermal process, hydrothermal methods and electro-deposition technique [48,49]. In this section we will introduce solvothermal and electro-deposition methods.

3.1.1. Solvothermal methods

Solvothermal is a synthesis method for growing single crystals from a non-aqueous solution in an autoclave at high temperature and high pressure. The syntheses carried out with this method showed a good control of the morphology, the crystallinity and the mono dispersion of nanoparticles [50]. Numerous syntheses of TiO_2 nanoparticles were carried out by solvothermal route, with or without surfactant. Figure 3 shows TEM and SEM images of TiO_2 nanoparticles synthesized by solvothermal technique. An example of TiO_2 nanoparticles synthesized by the solvothermal route, consists in preparing a solution of NH_4HCO_3, linoleic acid, triethylamine, cyclohexane and titanium butoxide $Ti(OBu)_4$ [51]. After continuous stirring, the mixture is immediately transferred to a teflon-lined stainless steel autoclave to be kept under 150°C for 24 hours. The obtained TiO_2 nanoparticles are stable for several weeks. The addition of an excess of ethanol causes TiO_2 precipitation at room temperature. Thus the TiO_2 can be re-dispersed in solvents such as chloroform, cyclohexane or linoleic acid. Recently, TiO_2 anatase nanoparticles with controlled size were synthesized by Ramakrishnan *et al.* using solvothermal method. They obtained TiO_2 nanoparticles with spherical shape and uniform size distribution (5 nm). The photodegradation efficiency of methyl orange and methylene blue dyes under the influence of UV-A light was 96% and 97%, respectively [48]. Moreover, solvothermal process improves different reactions, such as heat treatment reactions, phase transformation reactions, ion exchange, crystal growth and precipitation. Solvothermal technique has also some disadvantages including the need for expensive stainless-steel autoclaves, safety issues during reaction processes, and the impossibility of studying in-situ reactions due to their closed systems [52,53].

3.1.2. Electro-deposition technique

Electro-deposition technique has been also involved to synthesize TiO_2 nanoparticles [54]. In electro-deposition process an electric current is applied between a metal electrode (counter electrode) and the substrate (working electrode), through an electrolytic solution containing the metal ions. This process leads to an electron transfer between the substrate and the ionic species (redox reactions) which results in atoms deposition of that species onto the substrate. Several parameters affect the deposition's thickness and uniformity such as current density, deposition time, electrolyte agitation, composition of the

electrolyte and the type of polarization (continuous, pulsed) [55,56]. Jiang *et al.* used an electro-deposition technique for the deposition of TiO_2 nanoparticles on multi-walls carbon nanotube arrays which are acting as substrate. Their electrolytic solution was prepared by mixing 10 mM of H_2O_2, 3 M of KCl and 10 mM of $Ti(SO_4)_2$. The potential was fixed at 0.1 V and the deposition time was 30 min. The reaction temperature, time and pH were adjusted in order to control the size and morphology of TiO_2 nanoparticles. Electro-deposition technique was also involved to deposit metal nanoparticles on TiO_2 nanomaterial with the aim to improve the visible photocatalytic activity of TiO_2 [57]. Recently, Ag nanoparticles were successfully loaded onto TiO_2 nanotube arrays by Low *et al.* using a simple electro-deposition method. TiO_2 nanotube arrays and a Ti foil were immersed into an electrolytic solution rich in Ag^+ ions with a power supply of 3V and a deposition time of 1 minute. They concluded that the Ag nanoparticles promote the charge carrier migration on the TiO_2 nanotube arrays through unique near field effect. As a result, the photocatalytic CO_2 reduction performance under visible light of the TiO_2 nanotube arrays was greatly improved by Ag nanoparticles deposition compared to pure TiO_2 nanotube arrays [58]. Several studies have been devoted to the synthesis of nanomaterials by electro-deposition technique due to its low cost and low temperature feature. Despite these advantages, this technique has some limitations such as low deposition rates and limited usable substrates [59]. Nanoparticles of TiO_2-based materials were also synthesized by hydrothermal methods and they showed an enhancement in the visible light photocatalytic activity compared with pure TiO_2 such as Fe-TiO_2 [60], Co/Cu-TiO_2 [61] and S-TiO_2 [62]. This technique will be investigated in details in the next section.

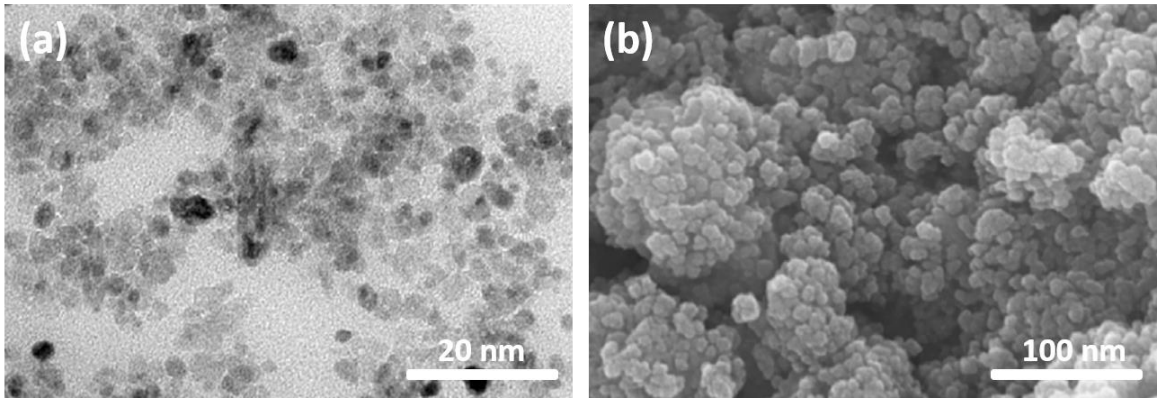

Figure 3: (a) TEM and (b) SEM images of 0D TiO_2 nanoparticles [48].

3.2. Synthesis techniques of 1D TiO_2 nanostructures

In recent years, much attention has been devoted to one-dimensional TiO_2 nanostructures such as nanofibers, nanorods, nanotubes and nanobelts for photocatalysis application due to their unique specific morphologies and good photocatalytic properties such as large specific surface area. Among several fabrication methods used to synthesis 1D, we will introduce the most common techniques: electrospinning, hydrothermal, electrochemical anodization, template assisted and sol-gel methods.

3.2.1 Electrospinning

Electrospinning is a versatile and cost-effective technique for the production of multi-functional nanofibers from various polymers, composites, sol-gels, ceramics etc. [63,64]. The basic principle of this technique is based on generating the direct movement of charged molecules by applying a high voltage to supply the ejection of a viscous liquid jet through a spinneret [3]. Electrospinning setup consists of three main components; (1) high voltage power supply, (2) syringe pump and (3) collector. Figure 4 shows the schematic view of an electrospinning experiment. When the electric field is created between the droplet of solution and the grounded collector, it overcomes the surface tension and the polymer jet is then created to begin the fiber formation [65]. The Taylor cone shape starts to be observed at the tip of the needle during the injection[66]. In electrospinning process, the morphology and uniformity of nanofibers are determined by considering a number of parameters which are investigated under two main parts: (a) polymer/solution properties such as molecular weight, viscosity, conductivity, surface tension; and (b) set-up parameters such as the electric field, the flow rate of solution and tip-to-collector distance. Moreover, the ambient conditions (temperature, humidity) may affect the formation of nanofibers [67,68]. In general, the elaboration of TiO_2 nanofibers using electrospinning involves the following three steps: (1) preparation of the electrospun solution with Titania precursor and a polymer template; (2) electrospinning of the solution to obtain the composite nanofibers, and (3) calcination of the as-prepared nanofibers to remove the polymer and to obtain the crystalline phase of TiO_2 nanofibers [69]. Nasr *et al.* reported on the elaboration of reduced graphene oxide rGO/TiO_2 composite nanofibers with different GO amounts using electrospinning technique.

They confirmed the decreasing of TiO_2 band gap energy from 3.2 eV to 2.9 eV due to the incorporation of GO sheets. In addition, they showed that the photocatalytic degradation of methyl orange under visible light by GO (2 wt.%)/TiO_2 was 6 times higher than that of commercial TiO_2 [70]. In order to increase the active surface area of TiO_2 nanofibers, different TiO_2-based composite and co-doped nanofibers were elaborated by electrospinning such as graphene-TiO_2[71], BN-TiO_2[72], ZnO/TiO_2[73], CuO/TiO_2[74], and Ag/TiO_2 [75]. The performances of these composites and co-doped materials for photocatalytic application have shown a significant enhancement compared with pure TiO_2 nanofibers. Even though electrospinning has a potential for industrial production, though it may not be suitable for mass production, due to the large standard deviations on nanofibers' diameter, and the restrict fiber mat purity by the presence of polymer beads.

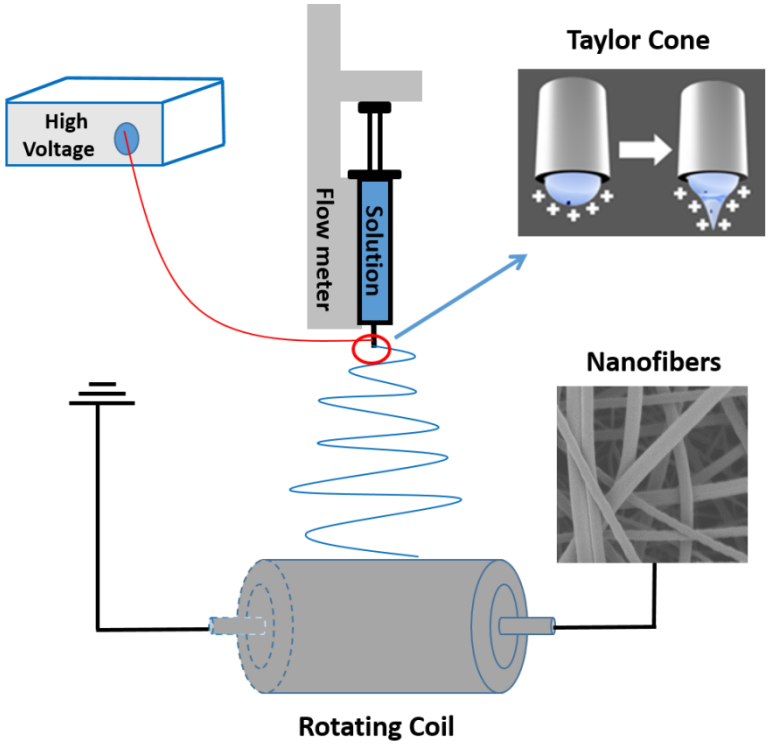

Figure 4: Schematic of the electrospinning process.

3.2.2. Hydrothermal methods

Hydrothermal technique is usually performed in a stainless steel vessel [76], this technique is the most commonly used for elaboration of 1D nanostructure [77]. It involves the growth of materials from aqueous solutions at high temperature (above the boiling point of water)

which produces high pressure [78]. Hydrothermal method is based on mixing the reagent with the precursor to be injected in the solvent which plays a double role: it accelerates the dissolution of the precursor as well as the reaction rate between the precursor and the reagent with the pressure and temperature increasing [79]. Tian *et al.*[80] report on the different 1D nanostructures elaborated by hydrothermal methods such as nanotubes [81], nanorods [82], nanowires [83] and nanobelts [84] as shown in Figure 5. It was found that the morphology and the length of the nanotubes affect the photocatalytic performance of TiO_2. The specific infrastructure of nanotube arrays promotes the photocatalytic reaction which improves the photocatalytic activity compared with Degussa P25 nanoparticles. In addition, this structure promotes the decomposition of organic pollutants due to the facile diffusion of pollutants into the TiO_2 nanotubes [85]. Despite the advantages of hydrothermal technique such as cost-effective, low energy consumption, simple equipment, chemical homogeneity and high dispersibility, the hydrothermal method has some disadvantages such as having long reaction time duration and producing non-uniform particle sizes of samples. One dimensional TiO_2 nanostructure was also synthesized using solvothermal method presented in the previous section. For example, Wang *et al.* managed to tailor the morphologies of TiO_2 from nanoparticles to nanoneedle and nanorod by combining the solvothermal method with a post annealing. They used to modify the reactant molar ratio, solvothermal temperature and reaction time in order to tailor the nanostructure of TiO_2 [86].

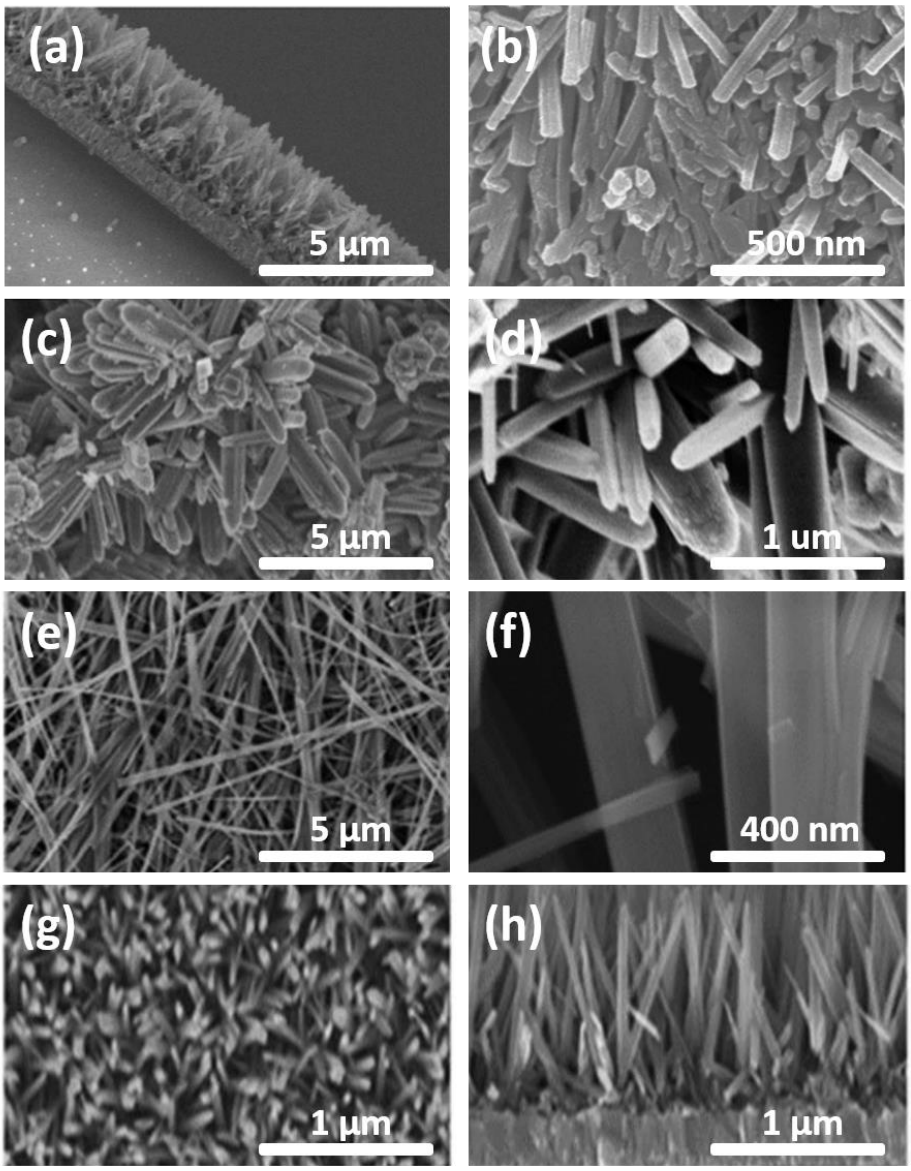

Figure 5 : Different morphology types of 1D TiO_2 nanostructures synthesized through hydrothermal methods: (a, b) TiO_2 nanotubes, (c, d) TiO_2 nanorods, (e, f) TiO_2 nanobelts, (g, h) TiO_2 nanowires, updated from references [80, 87, 88].

3.2.3. Electrochemical anodization method

The electrochemical anodization method can be employed to fabricate 1D TiO_2 nanostructures using one of three electrode configurations: a working electrode, a counter electrode and a reference electrode in an aqueous electrolyte. This low cost technique allows the formation of highly ordered and oriented TiO_2 nanotube and nanorod arrays [89]. Recently, Low *et al.*[58] fabricated highly ordered TiO_2 nanotube arrays through electrochemical anodization. Titanium (Ti) foils were cleaned in ethanol, and then were

electrochemically anodized in ethylene glycol solution at room temperature for 6 hours with a voltage of 30 V. Ag nanoparticles were loaded on TiO_2 nanotube arrays via electrochemical deposition. After washing, the nanotubes were annealed at 550°C for 2 hours. Figure 6 (a-b) presents the FESEM images of TiO_2 nanotube arrays as we can clearly observed the Ag nanoparticles on the top surface of the nanotubes. As results, they found that the photocatalytic CO_2 reduction performance under visible light was greatly enhanced due to the presence of Ag nanoparticles [58]. Electrochemical anodization was also used by Ye *et al.*[90] to fabricate self-organized TiO_2 nanotube arrays. The synthesis was conducted by electrochemical anodization in a two-electrode chemical cell connected to a power supply. A Ti foil was used as anode, and a stainless steel foil was used as cathode. The working distance between the electrodes was fixed to 2 cm. The anodization potential and the annealing temperature were modified in order to study their effects on the nanotubes. It was found that the anodization potential and the annealing temperature are the two key parameters which control the diameter and crystallographic composition of the anodic produced TiO_2 nanotubes, respectively. The self-organized TiO_2 nanotube arrays showed a good photocatalytic stability in the degradation of β-blocker metoprolol under UV-LED light [90]. The low cost electrochemical anodization method allows the formation of the longest tube length with a high surface area. However, it is a long time duration process and not suitable for mass production.

3.2.4. Template assisted method

1D titanium oxide nanostructure can be elaborated by template assisted method. This technique is usually used to synthesize aligned arrays of TiO_2 nanotubes and nanorods. Template assisted method is divided into two steps. The first one is based on an anodic oxidation of aluminum to obtain a very porous membrane (ZnO and silica can also be used as templates). The second step consist of using this membrane as a template to deposit TiO_2 tubes inside the pores[91,92]. For example, the TiO_2 deposition could be done by Atomic Layer Deposition (ALD) method which is a chemical deposition method in phase gaseous (ALD technique is explained in details in the next section). Vertically aligned TiO_2 nanotube arrays were fabricated by Lee *et al*. they combined atomic layer deposition with anodic aluminum oxide template (AAO)[93]. The AAO templates were introduced into the ALD chamber for TiO_2 deposition. TiO_2 deposition was performed at 150 °C using $TiCl_4$ and water as precursors.

The cycle was repeated for 300 times to obtain a TiO_2 layer with a thickness of 20 nm. After annealing at 450°C, TiO_2-coated AAO template was attached to a glass substrate. Then, the residual alumina layer of the AAO template was removed by treating in KOH solution and subsequently rinsing with deionized water. Finally, TiO_2 nanotube arrays are left on the transparent glass substrate. Top-view and cross sectional FESEM images of the obtained nanotubes show highly ordered and vertically aligned TiO_2 nanotubes (Figure 6 (c-d)). Lee *et al.*[94] reported a one-step templating synthetic strategy to prepare aligned TiO_2 nanotube arrays on Si substrate. ZnO nanorod arrays were obtained from an aqueous solution and were used as template. The deposition of TiO_2 and the selective etching of the ZnO template proceeded at the same time. They showed that the different thickness of TiO_2 sheaths, leading to the formation of nanotubes, can be precisely controlled by the deposition time[94]. The template assisted method presents several advantages such as providing precise control of the nanotube dimensions and yielding dense arrays of uniform nanotubes aligned on substrates to facilitate the incorporation into device structures. However, this process have some inconvenient for example (1) the dimension of nanotubes is limited by the geometric parameters of the membrane, (2) it is often difficult to achieve a good adhesion between the matrix and the substrate, and (3) the morphology of TiO_2 nanotubes can be modified during the dissolution process of the membrane [95,96].

3.2.5. Sol-gel method

Sol-gel process have also been used to obtain TiO_2 1D nanostructures such as nanorods, nanotubes and nanowires[97-99]. Sol-gel is a simple technique since it can be performed at low temperature. The principle of a sol-gel method consists of titanium alkoxide's hydrolysis, followed by a condensation, causing the formation of a colloidal solution. A gel is then obtained after a heat treatment. The reaction can be accelerated by addition of an acidic (HCl) or a basic (NaOH) catalysts. TiO_2 with high purity and high homogeneity can be obtained by Sol-gel method. The size, the shape and the crystalline phase of TiO_2 can be controlled by the pH, the solvent, the alkoxide and the catalyst[99-102]. Recently, Khore *et al.* have reported on the growth of N-TiO_2 1D nanorods using an aqueous sol–gel method followed by hydrothermal treatment[103]. Titanium tetra-isopropoxide, diethanolamine, and H_2O_2 were used as precursors for preparing an aqueous gel. They used

Trifluoroacetic acid (TFA) as a growth regulator and they studied its effect on the structure and morphology of N-doped TiO_2. FESEM images in Figure 6 (e-f) shows the uniform shaped of nanorods when N-doped TiO_2 gel was treated using 1%TFA. It was found that TFA plays a binary role by adjusting acidic pH of the solution mixture to control the morphology of TiO_2 and for selective growth of the rutile phase. N-doped TiO_2 with 1% TFA showed an excellent photocatalytic activity for the degradation of methyl orange and for H_2 generation under sunlight [103]. Sol-gel is a versatile method, it allows a better control of the structure such as porosity and particle size. This technique insures a better homogeneity and a high purity due to the mixing at a molecular level. Another advantage for this technique is a less energy consumption, there is no need to reach the melting temperature since the network structure can be achieved at relatively low temperatures. Despite all these advantages, sol-gel has some limitations including the high cost of precursors and the long duration process (the formation of gel is a slow process)[104].

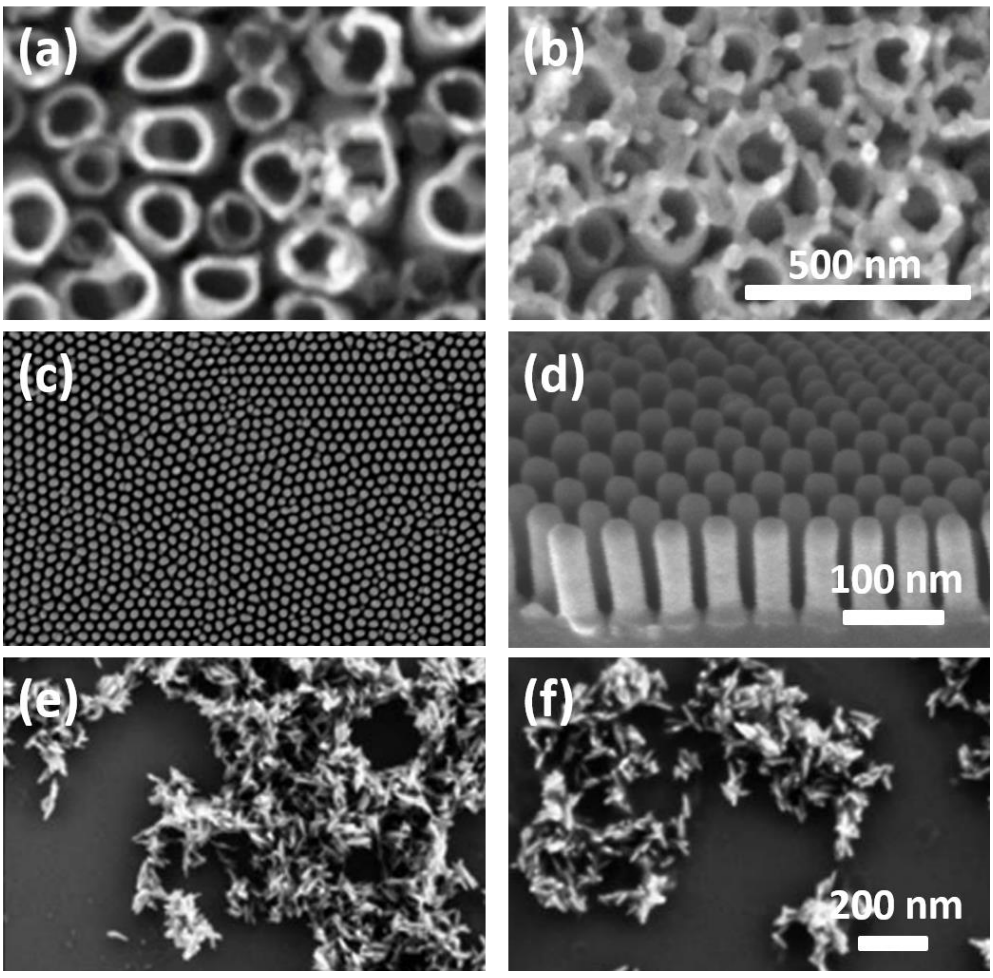

Figure 6: FESEM images of (a-b) top view of Ag/TiO_2 nanotube arrays synthesized by electrochemical anodization method [58], (c-d) top and cross-sectional of TiO_2 nanotube arrays elaborated using template assisted method [93] and (e-f) N-doped TiO_2 treated with 1%TFA synthesized using sol-gel method [103].

3.3. Synthesis techniques of 2D (thin films) TiO_2 nanostructures

Thin film deposition methods were largely investigated and used for laboratories study and industrial applications. These deposition methods can be divided into two categories: a liquid phase deposition including spin coating and dip coating and a gas phase deposition such as Chemical Vapor Deposition (CVD) and Atomic Layer Deposition (ALD).

3.3.1. Spin coating

Spin coating is one of the most common techniques for depositing thin films onto substrates. It is used in a wide variety of industries and technology sectors [105]. The advantage of spin coating is the ability to quickly and easily produce uniform films with a thickness ranging from a few nanometers to a few microns. A droplet of the precursor's solution is deposited at the center of the substrate. The substrate is then rotated at high speed in order to spread the solution by centrifugal force. Alternatively, the solution may be applied while the substrate is spinning [106]. The thickness, morphology and surface topography of the final film obtained from a particular material in a given solvent at a given concentration are highly reproducible. Due to the ability to have high spin speeds, the high airflow leads to fast drying. Different parameters affect the spin-coating deposition process such as rotational speed, viscosity, spinning time, molecular weight and concentration of the solutes [107]. Figure 7 shows SEM and TEM images of TiO_2 thin films synthesized by simple spin coating technique. Pan *et al.*[108] have grown highly ordered cubic mesoporous WO_3/TiO_2 thin films using spin coating method. The optimized doping amount was found at 4 mol % of WO_3 concentration and they showed that the long-range ordering of the mesostructure was appreciably organized. The enhancement of WO_3/TiO_2 photocatalytic activity in the decomposition of 2-propanol was ascribed to the surface acidity of the resultant mesoporous structures. Spin coating insures an easy control of the film thickness by

changing spin speed or using different viscosities. On the contrary, a large substrate cannot be spun at a sufficiently high rate in order to allow the film to thin. Another disadvantage of spin coating is its lack of material efficiency. Spin coating processes use only 2-5% of the material dispensed onto the substrate, while the remaining 95–98% is flung off into the coating bowl and disposed.

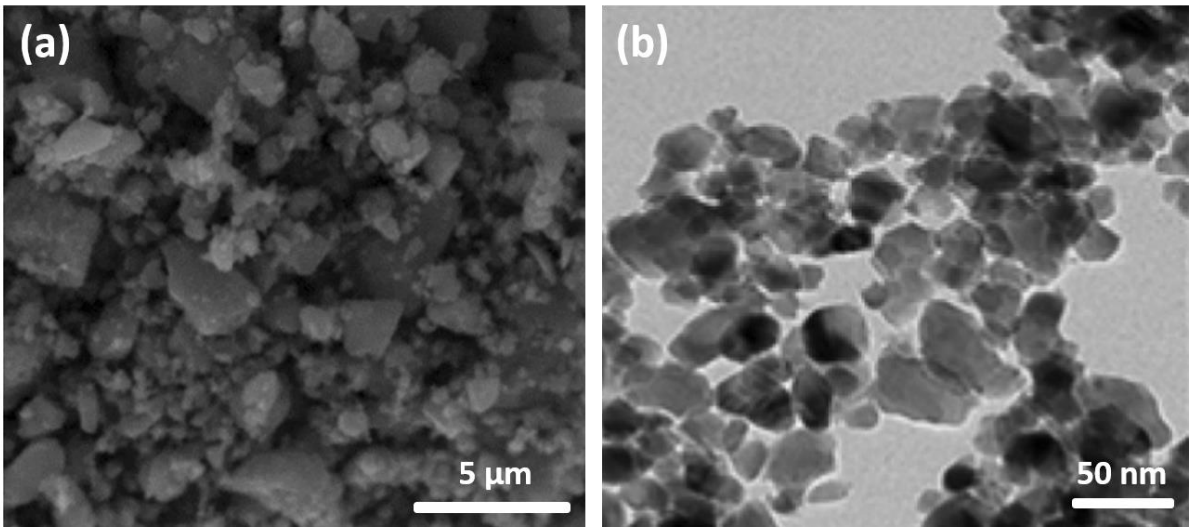

Figure 7: (a) SEM and (b) TEM image of the TiO_2 thin film synthesized by spin coating [109,110].

3.3.2. Dip coating

Dip coating is particularly well suited for the production of thin films because it allows the deposition of very homogeneous films on substrates of different sizes [111]. Moreover, this technique is perfectly controlled and it allows to properly adjust the microstructure (porosity, crystalline structure) of the deposition and to control their thickness [112]. This technique is based on the immersion of a substrate in the precursor's solution, fixing it for a while inside the solution then pulling it up at a constant speed. The thin layer deposits itself on the substrate while it is pulled up [113]. The assembly must be devoid of any vibration so that the surface of the solution remains immobile during the deposition in order to obtain a good quality deposition. The slightest disturbance during this step (immersion-pulling up) will cause horizontal streaks on the deposited film [114]. Different parameters should be controlled during the dip-coating process such as the immersion speed and the solution concentration and viscosity [115]. Several studies reported on the synthesis of TiO_2 and TiO_2 based materials via dip coating technique. SEM and AFM images show the morphology and the topography of the TiO_2 thin film synthesized by simple dip

coating technique (Figure 8). For example, Janczarek *et al.*[116] elaborated transparent thin films of Cu–TiO_2 on glass surface with different amounts of copper using the simple dip coating method. They concluded that the Cu-TiO_2 photocatalytic activity under visible light is correlated to the optimal content of copper (Cu/Ti ratio = 0.017). Despite the low cost and the easy process of dip coating, this sol gel technique is not able to elaborate completely densified and uniform coatings.

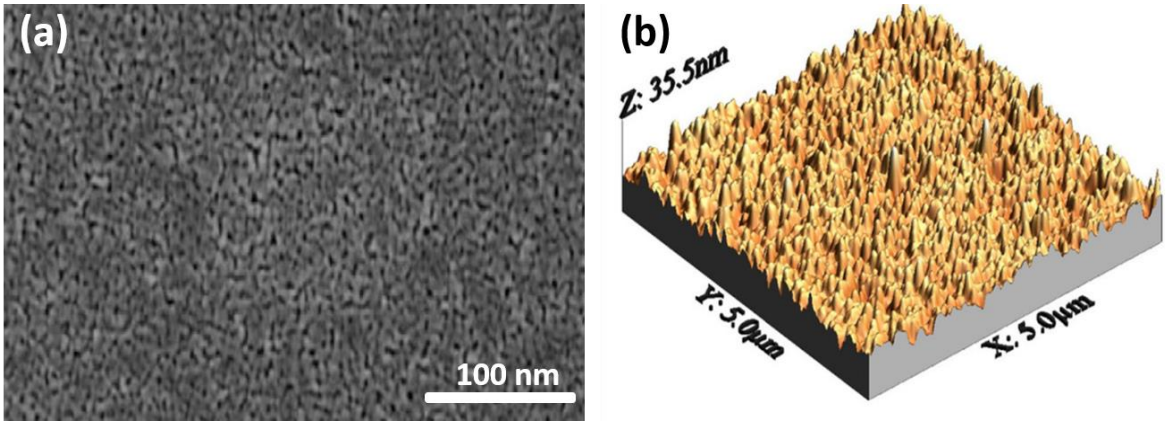

Figure 8: (a) SEM image of the TiO_2 thin film synthesized by dip coating [117] and (b) AFM images (topography channel) of the TiO_2 thin film [118].

3.3.3. Chemical vapor deposition (CVD)

Chemical Vapor Deposition (CVD) is a low cost technique that consists of growing a solid phase material from a gas phase containing the precursors of the materials [119]. In a typical CVD process, the substrate is exposed to one or more precursors which react and/or decompose in gas phase to produce the final film [120,121]. The CVD technique can be coupled with a plasma system as energetic activation instead of thermal activation and the process is then called Plasma Enhanced Chemical Vapor Deposition (PECVD) [122]. The thickness of the deposition and the size of particles can be controlled by the deposition time. Figure 8 shows the SEM images of TiO_2 thin films elaborated by CVD. For a deposition time of one minute, small round particles were obtained (Figure 9-a) with an average size of 20 nm and a deposition thickness of 253 nm, while for two minutes of deposition, large star-like nanoparticles were obtained (Figure 9-b) with an average size of 200 nm and a deposition thickness of 744 nm [123]. Yoshitake *et al.*[124] elaborated mesoporous titanium dioxide using chemical vapor deposition (CVD) of titanium isopropoxide followed by its decomposition with water vapor. They reported that CVD treatment improved the thermal stability of

template-extracted titania in air without changing the chemical composition. Recently, Youssef *et al.*[125] prepared single-oriented pure N-doped anatase films via PECVD technique using titanium isopropoxide as a precursor and NH_3 as a N-doping source. They concluded that N-doped TiO_2 film is an efficient photocatalyst for the photodegradation of stearic acid under visible light. CVD is widely used for laboratory and industrial applications due to the good coating ability in the micrometric range and low deposition temperature. Despite those advantages, the nanotechnology needs a deposition technique with nanometer resolution and 3D deposition ability.

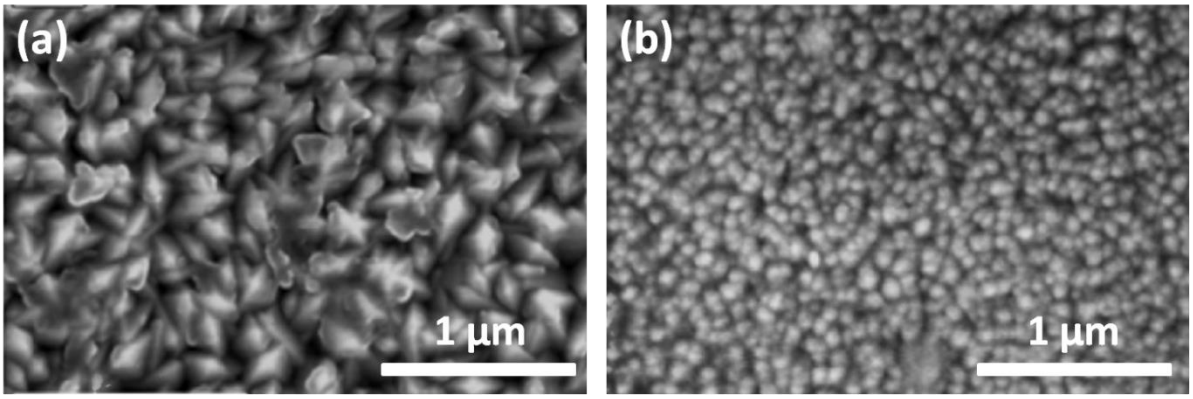

Figure 9: Scanning electron microscopy images of TiO_2 with different deposition times (a) 1 minute and (b) 2 minutes, updated from reference [123].

3.3.4. Atomic Layer deposition (ALD)

Many deposition techniques are available to deposit TiO_2 thin films on surfaces as explained above. These methods cannot deposit conformal films in the nano scale, the thick films created using these processes require significant precursor usage relative to alternate thin film solutions [126]. Atomic Layer Deposition (ALD) is gaining an increased attention in energy and environmental fields as promising method of surface modification and protection. [127-129] ALD is a vapor deposition method of ultrathin layers.[130-133] The originality of ALD is given to Professor Aleskovskii and his team in 1960 when they realized the deposition of TiO_2 from $TiCl_4$ and H_2O [134]. ALD is a deposition technique that derives from the CVD technique; it is based on 2 self-limiting reactions absolutely separated in gas phases. Two precursors A and B react on gas phases during the CVD deposition to produce a thin film on the surface of the substrate; the same precursors react separately in ALD with the substrate surface to produce a uniform coating. ALD is a multi-step gas phase adsorption technique that is an analog of a one-step CVD reaction. No other thin film technique can

approach the conformity achieved by the ALD on high aspect ratio structures [135-137]. One cycle including four steps is needed to be able to perform the 2 self-limiting reactions as presented in Figure 10. Step 1: introduction of the first precursor in the deposition chamber to react with the substrate surface and form a chemisorbed and physisorbed layer; Step 2: purge to eliminate both the physisorbed layer and the by-products of the reaction; Step 3: introduction of the second precursor to react with the chemisorbed layer resulting by the reaction of the first precursor with the substrate. As for the step 1, the chemisorbed and physisorbed layers were formed; Step 4: purge to eliminate both the physisorbed layer and the by-products of the reaction [138]. For photocatalysis application, many studies have been devoted to the formation of TiO_2 thin film photocatalysts [139]. In addition to thin films, various nanostructures of TiO_2 based materials have been obtained using ALD methods including Zn_2TiO_4 nanowires [140], ZnO-TiO_2 core-shell [141], Ag-TiO_2 nanocomposites [142] and Pt-TiO_2 nanoparticles [143]. The potential area of research is increasing in this field due to the accomplishment of ALD in deposition of conformal thin films over complex nanostructures in a precise manner. However, the long deposition time limits the use of ALD in large scale. Therefore, the fabrication in industrial scale is a crucial challenge posed on ALD which could be overcome either by scaling-up or quickening the processes.

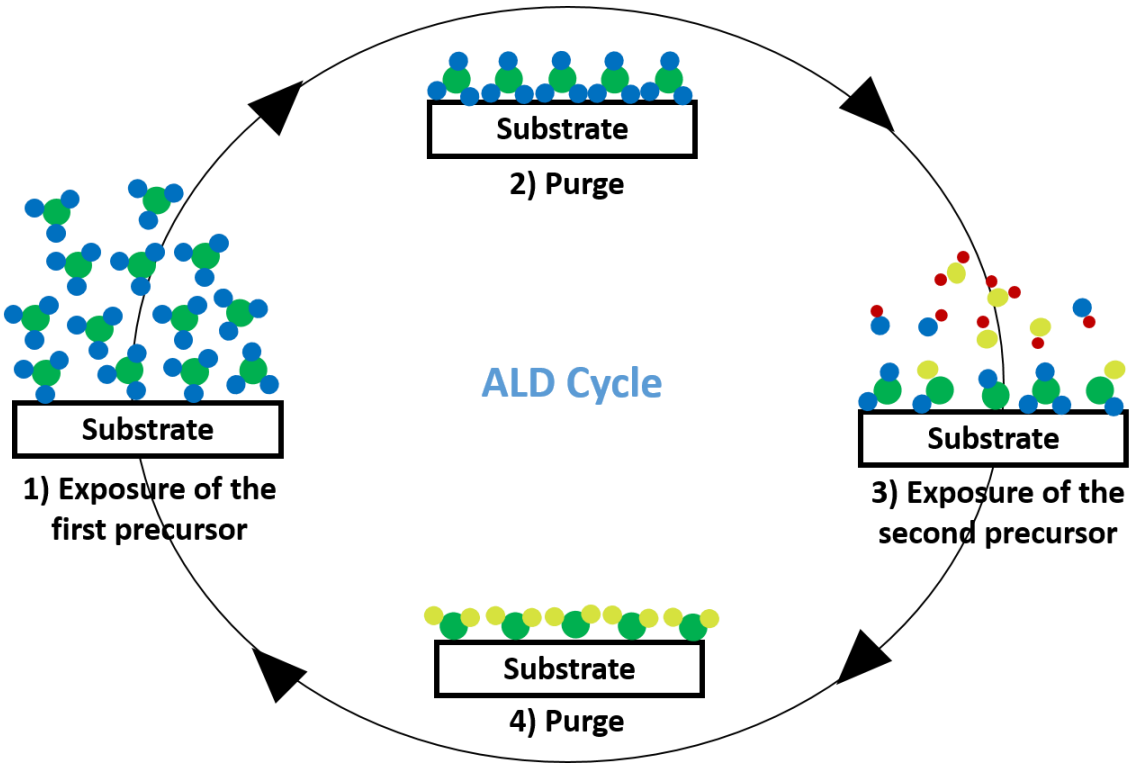

Figure 10: Schematics showing the growth process of ALD.

Since the nanostructure's morphology has a high impact on the photocatalytic activity, the most current synthesis techniques used to elaborate different morphologies of TiO_2 nanostructures have been presented. Each fabrication method has advantages and limitations, therefore Table 1 summarized the advantages and the disadvantages of all the synthesis techniques presented above. In the next section, we will discuss the different photocatalysis parameters and how they can be controlled and/or modified in order to improve the photocatalytic performance of TiO_2.

Table 1: Advantages and disadvantages of the different fabrication methods.

Fabrication method	Advantages	Disadvantages	Ref
Solvothermal	- Good control of the: Morphology Crystallinity	- Critical reaction conditions: High pressure High temperature - High cost equipment	53
Electro-deposition	- Low cost - Low temperature feature	- Low deposition rate - Limited usable substrates	59
Electrospinning	- Cost-effective - Industrial application - Formation of nanofibers with high surface area	- Large standard deviations of nanofiber's diameter - Restrict fiber mat purity	144
Hydrothermal	- Low energy consumption - Simple equipment - Chemical homogeneity	- Long reaction time duration - Non-uniform particle sizes	86
Electrochemical anodization	- Low cost - Longest tube length - Formation of tube with high surface area	- Not suitable for mass production - Long time duration process	90
Template assisted	- Control of nanotube dimensions - Yielding dense arrays of uniform nanotubes	- Complicated process - Limitation of nanotube's dimension by the geometric parameters of the membrane	96
Sol-gel	- Control of the porosity and particle size - Good homogeneity and high purity - Low energy consumption	- High cost of the precursors - Long duration process	103
Spin-coating	- Easy control of the film thickness - Uniform films	- Lack of material efficiency - Not suitable for mass production	109
Dip-coating	- Low cost - Easy process	- Not able to produce densified and uniform coatings	117
Chemical vapor deposition	- Low deposition temperature - Uniform coating in the micrometric range	- Not able to produce conformal films in the nano-scale range	125
Atomic layer deposition	- Deposition of conformal thin	- Long deposition time	145,146

	films in a precise manner in the nano-scale range - Low energy consumption	- Not suitable for mass production for large scale application	

4. Photocatalysis operating parameters

The rate of a photocatalytic reaction could be affected by external factors called "the operating or extrinsic parameters" such as the pH of the solution, the initial concentration of the organic compound, the catalyst concentration, the oxygen content and the temperature[25,147,148].

- (1) Concentration of the catalyst: previous studies showed that the catalyst concentration is proportional to the concentration of the electron-hole pairs (generated during the process). Actually, an increase in the amount of catalyst increases the number of active sites on the photocatalyst surface and thus improves the photoreaction rate [149,150]. It was also found that the reaction rate increases with the concentration of catalyst until a maximum constant value (limit concentration) corresponding to the total absorption. Above this limit concentration, the photoreaction rate could even decrease [151,152].
- (2) Initial concentration of the pollutant: as in any chemical reaction, the reaction is limited by the concentration of one or more reagents in a heterogeneous medium as follow:

$$r = \frac{dC}{dt} = \frac{kKC}{(1+KC)} \qquad \text{(Equation 6)}$$

In general, the behavior of Langmuir-Hinshelwood type is observed, where r is the degradation rate of the reagent, k represents the kinetic reaction constant, K the adsorption equilibrium constant and C the concentration of the reagent in the aqueous medium. For low value of C (KC << 1), the reaction follows a first order apparent behavior whereas for high value of C (KC >> 1) the reaction follows a zero order behavior [25,153]. Several researches affirmed that the photodegradation efficiency decreased when the initial concentration of the pollutant increased. In fact, more pollutant molecules were adsorbed on the surface of the catalyst, thus the generation of OH radicals at the catalyst surface was reduced because the active sites were occupied by pollutant cations [154,155].
- (3) Oxygen content in the medium: oxygen (from air flow) reacts with the electrons on the surface of the semiconductor and allows the balance of charges to be maintained [150]. Huang

et al.[156] studied the effect of adding H_2O_2 on the decolorization of methyl orange. They found that the decolorization rate was increased with the increase in H_2O_2 concentration. They reported an optimum concentration of 1.2 mM/L H_2O_2 for photocatalytic decolorization of methyl orange solution by Pt modified TiO_2.

- (4) The pH value plays an important role on the charge surface of both semiconductor and pollutant. On the one hand, it can modify the size of the particles in the aqueous medium; on the other hand, it can modify the adsorption of the pollutant on the surface of the semiconductor. The effects of pH on the photocatalytic degradation of the pollutant have been studied by many researchers and they found that the degradation rate of pollutants is increasing with the decrease in pH [157-159].

- (5) Temperature: previous studies showed that the photocatalytic system does not require heat input because it is a photonic activation process. The majority of photoreactions are not sensitive to small variations of temperature. The decrease in temperature promotes the adsorption which is a spontaneously exothermic phenomenon. When the temperature rises above 80°C, the exothermic adsorption of the pollutants is disadvantaged. Actually, the photocatalysis experiments using high power lamps are equipped with cooling system in order to maintain the temperature of the whole system at 25°C [160,161].

5. Modification of TiO_2 properties

One of the limitations of the photocatalytic process in the presence of TiO_2 is the fast recombination of charge carriers [162]. This recombination reduces the quantum efficiency of the photocatalytic process of TiO_2. On the other hand, the non-absorption of visible light limits its applications in sunlight [163,164]. In order to improve the photocatalytic activity of TiO_2, several researches have been carried out on the modification of TiO_2 properties. In this section, we will briefly introduce the metal-doping, surface modification with metal elements, modification with non-metal elements, coupling TiO_2 with other semiconductors and design of multiple components.

5.1. Metal-doping

Hoffman *et al.*[165] have shown that the substitution of Ti atoms with metallic atoms modifies the absorption of TiO_2 by introducing localized energy levels between the valence band and the conduction band of TiO_2. The energy of these levels as well as the distribution

and the concentration of dopants in the semiconductors, play an important role in the photocatalytic process. They introduce extrinsic band gap with lower energy, facilitate the electron-hole separation and the hosting of active sites on the surface of TiO_2 [166]. To overcome the limitations of TiO_2 photocatalyst, it was doped with different metals such as iron, cobalt, chrome, copper and gold[167]. Iron doping was used to improve the photocatalytic properties of TiO_2. The substitution of Ti atoms by Fe atoms in the TiO_2 network is possible thanks to the similarity of their ionic radii. DFT simulation studies were carried out by Asai *et al.*[168] and more recently by Yalçin *et al.*[169]. In both studies, a slight shift in the energy levels of VB and CB and the creation of intermediate levels are predicted: these results are based on the interaction of the iron 3d orbitals with the TiO_2 conduction band. Therefore, Fe-TiO_2 nanoparticles are able to absorb visible radiation. Zhu *et al.*[170] reported on the synthesis of chromium-doped titanium dioxide by combining the two techniques sol-gel and hydrothermal. From atomic absorption flame emission spectroscopy (AAS) and X-ray photoelectron spectroscopy (XPS), it was found that due to the high surface area and the strong electrostatic interaction Cr^{3+} ions firstly adsorbed on the surface of TiO_2 gel. Then the Cr^{3+} ions diffuse gradually into the bulk of TiO_2 grains by injecting into the Ti^{4+}vacancy or substituting Ti^{4+} ions in crystallization of TiO_2 during the hydrothermal treatment. Diffuse reflectance spectra showed an enhanced absorption in the visible region (from 387nm to 450 nm) after chromium ions doping. This extended absorbance was attributed to the charge transfer band ($Cr^{3+} \rightarrow Ti^{4+}$). As results, Cr^{3+} doping promotes the charge separation, reduce the band gap of TiO_2 and enhance its photocatalytic activity under visible light[170]. However the positive effect of metal-doping on the photocatalytic process[171], some studies confirm that metal-doping can act as electron-hole recombination centers which are detrimental to the photocatalytic activity [172].

5.2. Surface modification with metal elements

Metal nanoparticles such as Pt, Pd and Ag have been used to modify the properties of TiO_2 [17,173]. It was found that the surface modification by metal nanoparticles (acting as photosensitizers) improves the photocatalytic activity of TiO_2 in the visible range. Among all the noble metals, Ag is promising for extensive applications because of its low cost, facile preparation and antibacterial properties [174]. Until now, many strategies including chemical reduction, UV irradiation, hydrothermal method and electrospinning have been investigated

to synthesize different Ag/TiO_2 nanostructures for photocatalytic application[75,175-178]. They reported that the deposition of Ag nanoparticles can largely prevent the recombination of photo-induced electron-hole pairs in TiO_2. On the other hand, they demonstrated that the fact of introducing Ag leads to a red shift of TiO_2 absorption edge wavelength, thus to an enhancement of the photocatalytic activity of TiO_2 under visible light irradiation. Figure 11 shows STEM and SAED images of pure TiO_2 nanofibers and Ag–TiO_2 nanofibers. The successful incorporation of Ag nanoparticles in TiO_2 nanofibers is clearly seen in Figure 11-c (red dashed circles). In addition to the diffraction rings of anatase phase, an extra diffraction ring can be seen in the Ag-TiO_2 pattern indicating the presence of the crystalline Ag in the (111) orientation (Figure 10-d) [75,174]. Wang *et al.*[179] have shown that the deposition of Pd on the surface of TiO_2 significantly decreases the rate of depolarization of the particles to such an extent that the accumulation of negative charges in the particles becomes zero. This phenomenon is attributed to the improvement of the mechanism of capture and transport of photo-electrons by Pd to adsorb O_2. With the decrease of electrons in the particles, the probability of charges recombination decreases and the photocatalytic process is more efficient [179-181]. The enhancement of the photocatalytic activity with Pt-TiO_2 as photocatalyst was also studied and explained as follow: the electrons are transferred to the Pt while the deficiency accumulates at the Pt/TiO_2 interface leading to the charges separation and thus reducing the recombination of the electron/hole pairs [182,183]. The deposition of metals such as Cu[184], Au[185] on the TiO_2 surface enhances its photocatalytic activity, In fact, these nanoparticles act as electron sensors and improve the separation of charges [186]. Cu-TiO_2 have been frequently applied in antibacterial treatments, and in CO_2 photoreduction reactions[184]. Although metal-TiO_2 catalysts have been an efficient photocatalyst under visible light, they still suffer from multiple competitive disadvantages, including their high cost, susceptibility to gas poisoning, and detrimental effects on the environment. The cost-effectiveness needed by industrial application usually causes their replacement by more economical transition or non-metal elements.

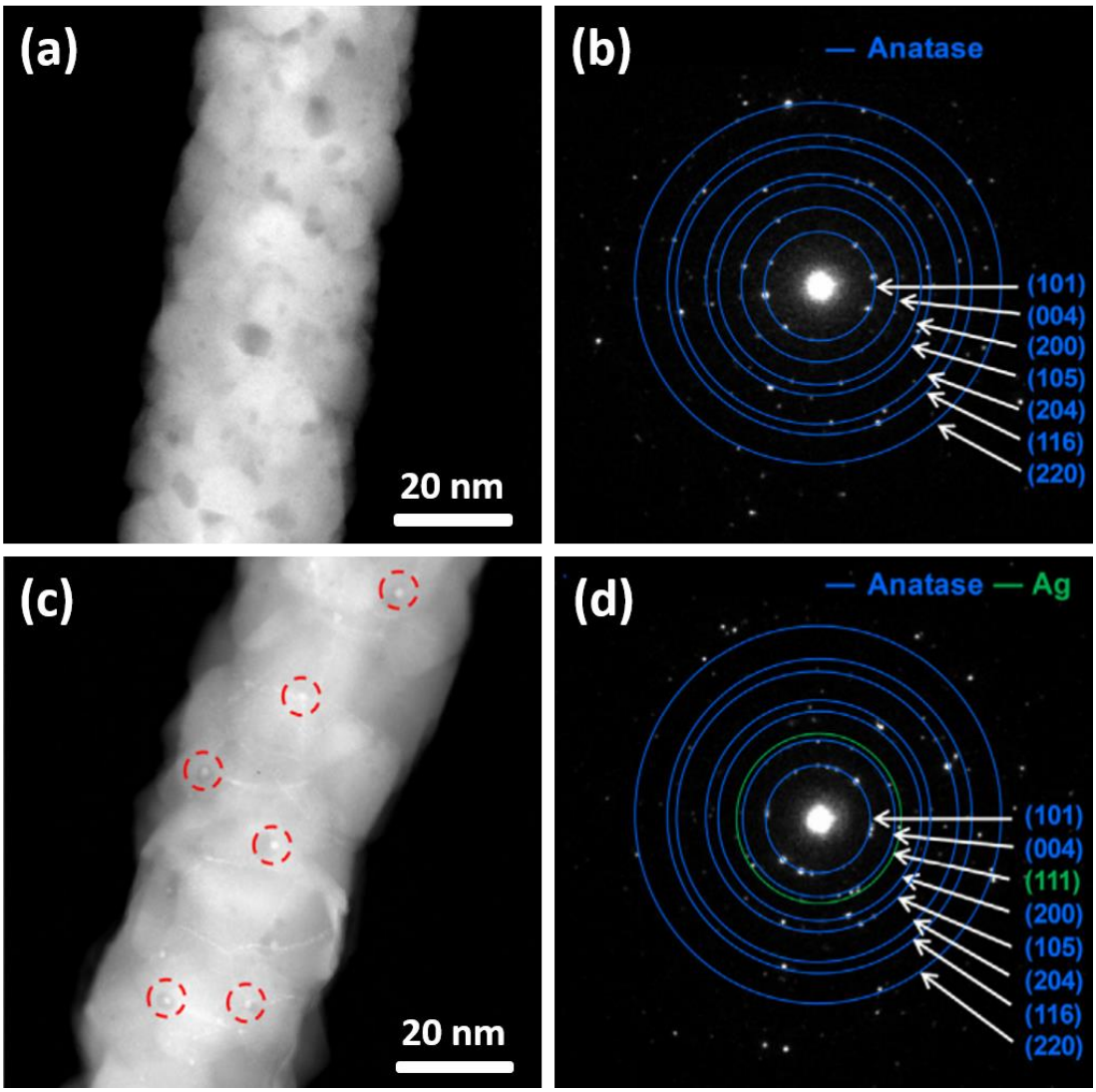

Figure 11: STEM and SAED images of pure TiO_2 nanofibers (a-b) and 0.5 at.% Ag–TiO_2 nanofibers (c–d). Red dashed circles in STEM images indicate Ag nanoparticles in TiO_2 nanofiber bulk. Blue and green circles in SAED images indicate anatase TiO_2 and metal Ag diffraction peaks, respectively, updated from reference [75].

5.3. Modification with non-metal elements

Due to problems associated with metal-photocatalyst, modification with non-metal elements were studied comprehensively in the hope of achieving visible light active stable titanium dioxide [187,188]. The fact of introducing these elements in the TiO_2 network reduced the excitation energy of TiO_2 either by reducing the band gap energy or by creating intermediate energy levels between the valence band and the conduction band [189,190].

5.3.1. Modification with carbon (CNT, graphene, graphene oxide)

Previous studies showed that non-metal doping is able to shift the optical absorbance of TiO_2 to the visible region [191,192]. Recently, a lot of attention has been devoted toward TiO_2 doped with carbon materials[193]. Etacheri *et al.*[194] have reported that the observed visible light activity is due to the substitution of carbon atoms in the TiO_2 photocatalyst which introduces a new state (C 2p) close to the valence band of TiO_2 (O 2p). C-doped TiO_2 offer high active surface area which is one of the important parameters leading to the increase of the photocatalytic activity. Several studies were focused on Carbon nanotubes (CNT)/TiO_2 nanocomposites [195,196]. CNT is considered as a remarkable material due to its unique hollow structure, high electrochemical stability, strong adsorption and high surface-to-volume ratio. It also has an excellent charge transfer ability that contributes to restrain the combination of electron–holes in TiO_2 [195,197]. Single-walled carbon nanotubes (SWCNTs) have shown a synergy effect on enhancing photoactivity over a mixture of SWCNTs and TiO_2 [198]. On the other hand, previous studies have also demonstrated that multi-walled carbon nanotubes (MWCNTs) could enhance the visible-light-driven photoactivity of TiO_2 by acting as a photosensitizer and promoting the charge transfer in the MWCNT-TiO_2:Ni composites [199]. The presence of MWCNT in the MWCNT/TiO_2 composites is clearly observed in SEM image of Figure 12-a (represented in yellow circle). The structure of the nanotubes and the presence of MWCNT in the composite were also detected by TEM image. From Figure 12-b, we can make a distinction between MWCNT and TiO_2 nanotubes (TNT), where MWCNT are intimately bound to the TNT surfaces (yellow arrows) [200].

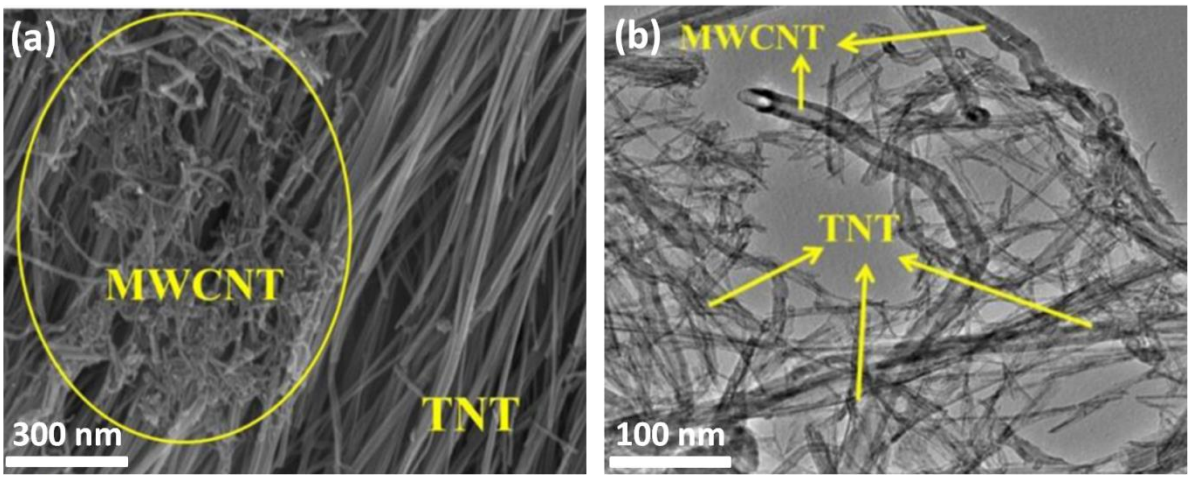

Figure 12: (a) SEM and (b) TEM images of MWCNT/TNT composites, updated from reference[200].

In 2004, the synthesis of graphene was reported for the first time [201]. Graphene is a one-atom-thick sheet of sp^2 bonded carbon atoms packed into a 2D honeycomb structure [202,203]. Graphene has excellent thermal conductivity, large specific surface area, high electron mobility and good mechanical strength. These properties of graphene make it an ultimate candidate material for enhancement of TiO_2 photoreactivity [204]. Previous studies concluded that graphene enhances the transport of electrons and suppresses the recombination of the electron-hole pairs. They demonstrated that with the use of graphene-TiO_2 composite (with small amount of graphene) agglomeration of TiO_2 can be avoided so that higher surface area can be maintained and there will be more active sites for the degradation of pollutants. Graphene-TiO_2 composite were doped with different metal and non-metal ions in order to improve the visible-light photocatalysis activity of TiO_2 [205,206].

Due to the high cost of graphene production, most of researchers choose to work with reduced graphene oxide which can be produced at low cost [207,208]. Graphene oxide (GO) is usually obtained by the oxidation of graphite using the famous Hummers' method and followed with an exfoliation step (high power ultrasonication) [209]. Reduced graphene oxide (removal of some oxygen functionalities) can be obtained by thermal or chemical reduction of graphene oxide [210]. Several advantages motivated the researchers to use rGO or GO/TiO_2 composites to enhance the visible light photocatalytic activity of TiO_2. For example, GO has an excellent carrier mobility, thus the photoelectrons will be rapidly transferred to the GO layers, which reduce the probability of electron-hole recombination. The large surface area of graphene oxide will offer more active adsorption sites of pollutants. In addition, the band gap of graphene oxide can be tuned (from 2.7 to 1.15 eV) by varying the oxidation level (reduced graphene oxide) [211-213]. The key of an effective visible light photocatalytic activity is to shift the absorbance of TiO_2 from UV range to the visible range by reducing the band gap energy of TiO_2. Many researchers have proved that using graphene oxide as a dopant for TiO_2 will lead to the Ti-O-C bond formation and therefore introduces lower band gap energy which will improve the visible light photoactivity of TiO_2, as shown in Figure 13 [214,215].

Since the surface complexity, the crystalline phase, the porosity and the size of photocatalyst play an important role in the photocatalysis process enhancement, different morphologies of GO/TiO_2 structures were successfully elaborated [216-218]. Lavanya *et al.* [210] fabricated reduced graphene oxide wrapped with mesoporous TiO_2 nanofibers using the simple electrospinning technique and easy chemical reduction. They demonstrated that the reaction area and the adsorption of dye were increased due to the high surface area of the rGO. As result, the photocatalytic activity of the composites is enhanced compared to TiO_2 nanofibers alone. Li *et al.*[219] showed that the porosity improves the utilization rate of the visible light because the light enters the porous TiO_2 nanotubes and is repeatedly reflected inside the nanotubes until it is completely absorbed.

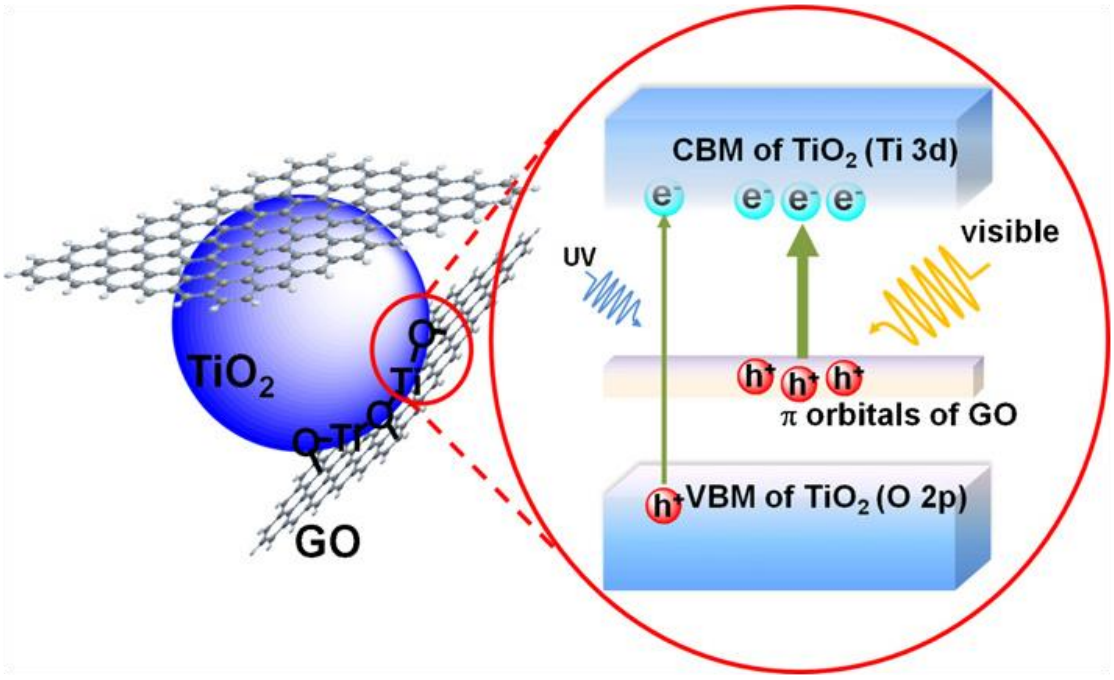

Figure 13: Ti–O–C bonding formed through interaction between unpaired π electrons on GO with Ti atoms surface of TiO_2. This bonding narrows the band gap of TiO_2 and extends the light absorption range of TiO_2[220].

5.3.2. Nitrogen doping

Due to its high stability and small ionization energy, nitrogen was also an element of increased interest over the years with several publications focusing on the N doped TiO_2 for visible light photocatalysis[221-223]. There are three different explanations regarding modification mechanism of TiO_2 doped with nitrogen:

- (1) Impurity energy levels: Wang *et al.*[224] suggested that after nitrogen doping, N element substitutes the O element in the lattice of TiO_2 and forms isolated impurity energy levels above the valence band. They proposed that Irradiation with UV light excites electrons in both the VB and the impurity energy levels, but illumination with visible light only excites electrons in the impurity energy level.
- (2) Band gap decreasing: Cao *et al.*[225] found that due to their close energies, N 2p state hybrids with O 2p states, leading to the band gap narrowing which renders N-TiO_2 active under visible light.
- (3) Oxygen vacancies: Ihara *et al.*[226] affirmed that oxygen vacancies, formed in the grain boundaries, are stabilized by the presence of nitrogen. As a result of charge compensation, they improve the visible light response. Till now, no study has demonstrated completely the exact chemical states of N species that are responsible for achieving visible light photocatalytic activity of TiO_2.

Figure 14 shows a possible mechanism of photocatalytic reactions of $\dot{O}^-$ radical and the schematic band structure of N-doped TiO_2 under visible light irradiation. The electron transfers directly into the conduction band of TiO_2, reducing O_2 to form superoxide ions (O_2^-). The hole (h^+) then reacts with OH^- group to produce ȮH radical, which are responsible for the degradation of the pollutants under visible light irradiation [227,228]. Cheng *et al.* reported on the elaboration of N doped TiO_2 nanoparticles with a photodegradation efficiency up to 90% for the removal of rhodamine B. The enhanced visible photocatalytic activity was attributed to the narrowing of the band gap energy. The successful N doping was detected by XPS. Figure 15-a shows a comparison of the XPS spectra of pure TiO_2 and N doped TiO_2 nanoparticles. For pure TiO_2 sample, C, O and Ti elements were detected by XPS. On the contrary, for N doped TiO_2 sample C, O, Ti elements and a small amount of N element were detected. In fact, the first peak at binding energy of 401.2 eV (Figure 15-b) was assigned to the Ti–O–N bond, while the other was attributed to the anionic N in the form of N–Ti–O bond [229].

As reported for metal-doping, non-metal doped TiO_2 has also its own problems. For example, the doping of nonmetals into the lattice of TiO_2 usually results in the formation of oxygen vacancies in the bulk which can act as massive recombination centers of photo-induced electron-hole pairs and therefore limits the visible light photocatalysis efficiency of

doped TiO_2. The stability of non-metal doped TiO_2 is also a concern regarding the long-term photocatalytic stability. Therefore, other research focuses on the coupling of two semiconductors as it will be discussed in the following section.

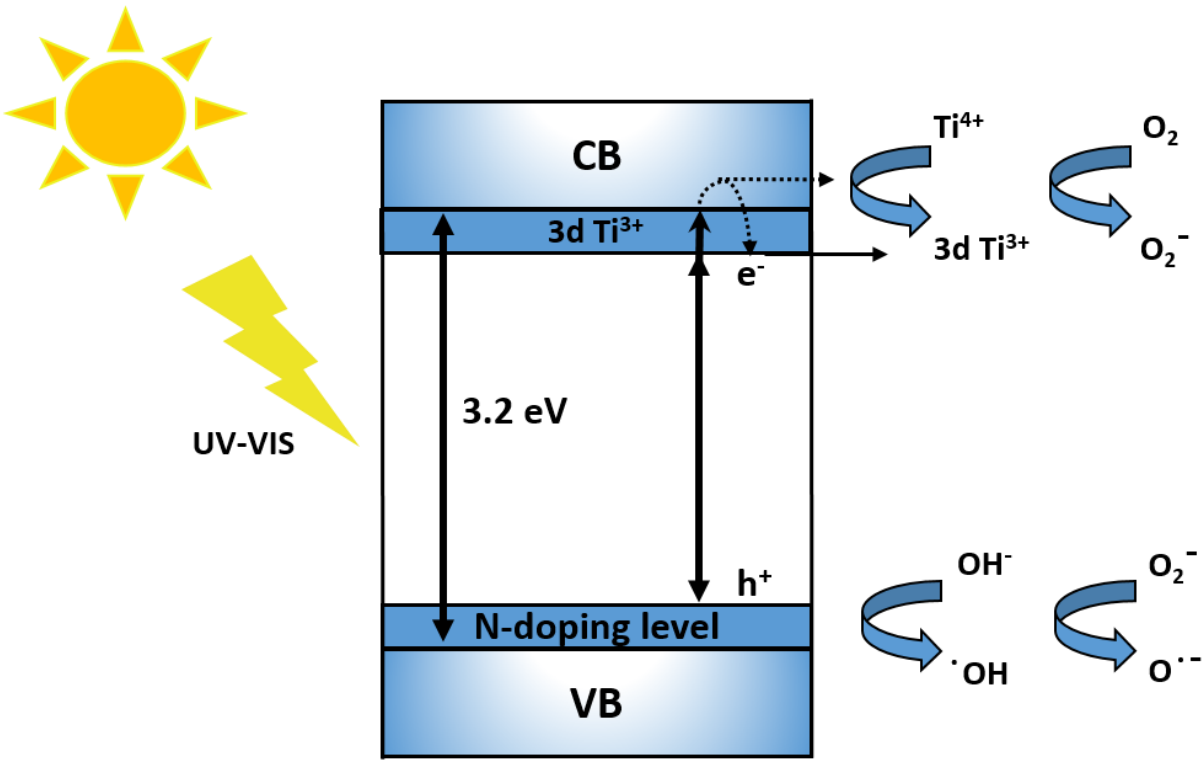

Figure 14: A possible mechanism of photocatalytic reactions of $\dot{O}^-$ radical and the schematic band structure of N-doped TiO_2 under visible light irradiation, updated from reference [222].

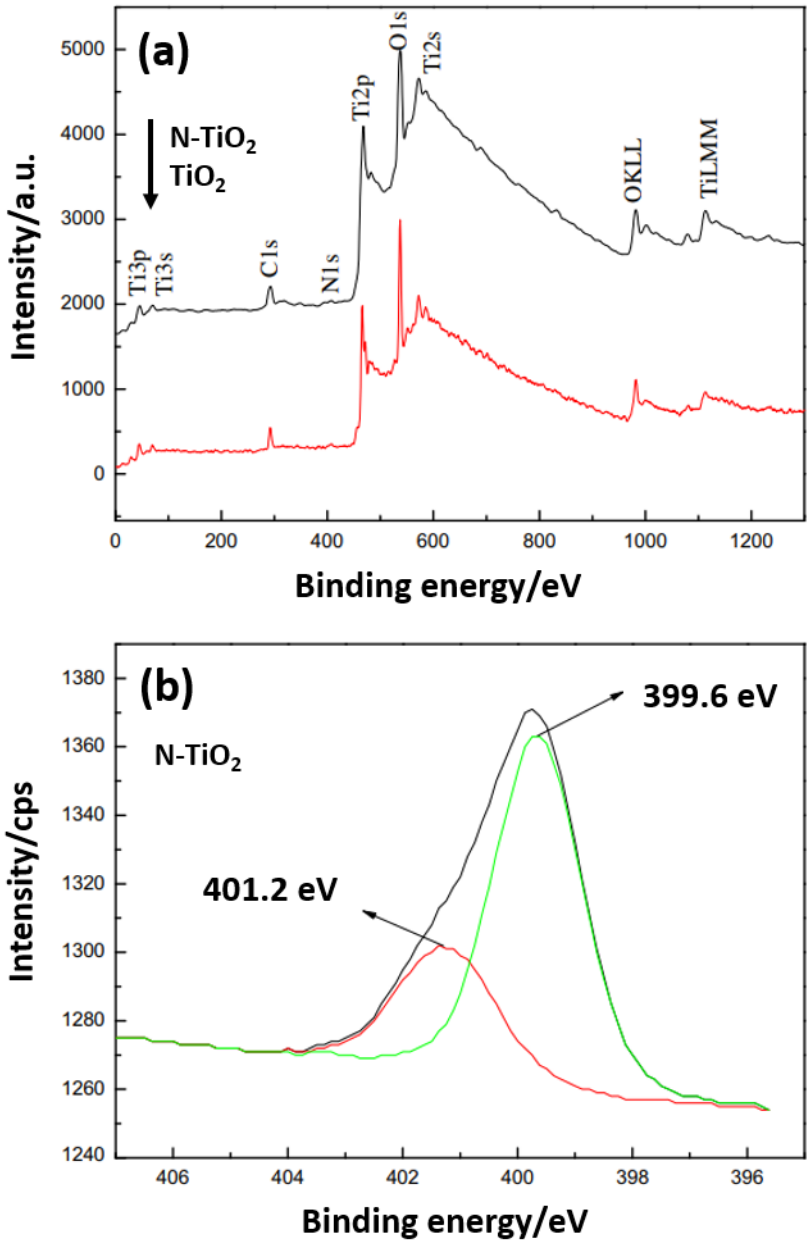

Figure 15: Global XPS of (a) pure TiO_2 and (b) N doped TiO_2 photocatalyst, updated from reference [229].

5.4. Coupling TiO_2 with other semiconductors

During the formation of an interface between two different semiconductor's phases, the difference in energy between the conduction and valence bands of the two phases may allow the irreversible spatial separation of the charge carriers as long as this difference in energy is sufficiently large[230]. In addition to the importance of these interfaces between crystalline phases for the efficient separation of charge carriers, the interfaces' structure

plays an important role for the interfacial transfer process efficiency [231]. For visible light photocatalysis, the nanoscale coupling is between TiO_2 and another small band gap semiconductor such as WO_3, SnO_2, FeO_3 and CdS[232-235]. The small band gap semiconductor allows the absorption band of TiO_2 to be shifted toward visible wavelengths. These semiconductors with a smaller band gap absorb a part of the visible light and can serve as sensitizers for TiO_2. Thus, many coupled photocatalysts have been used in the field of pollutant degradation [236]. The coupling between TiO_2 and another semiconductor at the nanometric scale leads to the formation of an interface between the two semiconductors, called heterojunction. The existence of this interface under optimum conditions will make it possible to increase the efficiency of the photocatalytic process by reducing the probability of the photogenerated charges recombination through their spatial separation on the two semiconductors. Therefore, we must consider the relative positions of the energy levels of the valence and conduction bands of the two semiconductors [237]. Figure 16 presents the semiconductors configuration in which a vectorial transfer of photogenerated electron−hole, between corresponding band levels, ensures a spatial separation between them. Previous study shows that it is necessary that the conduction band of TiO_2 be more anodic than the corresponding band of the sensitizer. Thus, under visible irradiation, only the sensitizer is excited and the generated electrons will flow into the conduction band of the adjacent TiO_2 (Figure 16-a). Besides, if the valence band of the sensitizer is more cathodic than that of TiO_2, the holes will be lower in the valence band of the sensitizer (Figure 16-b) [231]. Subsequently, this phenomenon has been widely studied and discussed. Moreover, for an effective vectorial phenomenon under visible light, the following steps are required: (1) the sensitizer should have a strong absorption threshold in the visible region; (2) the conduction band edge potential of the sensitizer should be higher than the TiO_2 conduction band to facilitate the smooth electron transfer; (3) simultaneous irradiation and excitation of the two semiconductors; (4) intimate contact between the two types of semiconductor particles. Thus, this physical separation of the photogenerated charges will make it possible to increase their lifetime and improve the efficiency of the visible light photocatalytic phenomenon [238]. Li *et al.*[239] prepared CdS (2.4 eV) sensitized mesoporous TiO_2 photocatalysts. Both the conduction band and the valence band of CdS are higher than their counterparts in TiO_2. The presence of CdS in the TiO_2 framework extended its

photoresponse to the visible light region by accelerating the photogenerated electron transfer from the inorganic sensitizer to TiO_2. High photocatalytic activity has been recorded toward the degradation of organic compounds under visible light. Recently, Khan *et al.* prepared TiO_2/WO_3 coupled semiconductors via facile sol-gel method. Figure 17-a shows the spherical morphology of TiO_2 nanoparticles and the needle-like structure of WO_3. The EDX elemental mapping presented in Figure 17-b reveals the homogeneity of the sample and confirms that Ti, O and W are evenly distributed over the entire area of the sample. They reported that this structure greatly improves the photocatalytic activity of TiO_2 (photodegradation of methylene blue) due to the difference in band potential of the semiconductors. In fact, electrons diffuse from the conduction band of TiO_2 to that of WO_3 which increases the lifetime of electron-hole pairs and decreases the recombination rate [240]. Despite all these advantages for using coupled semiconductors, the presence of a large number of non-passivated or partially passivated surface states act as trap centers for holes and electrons, leading to a decrease in the photocatalytic activity.

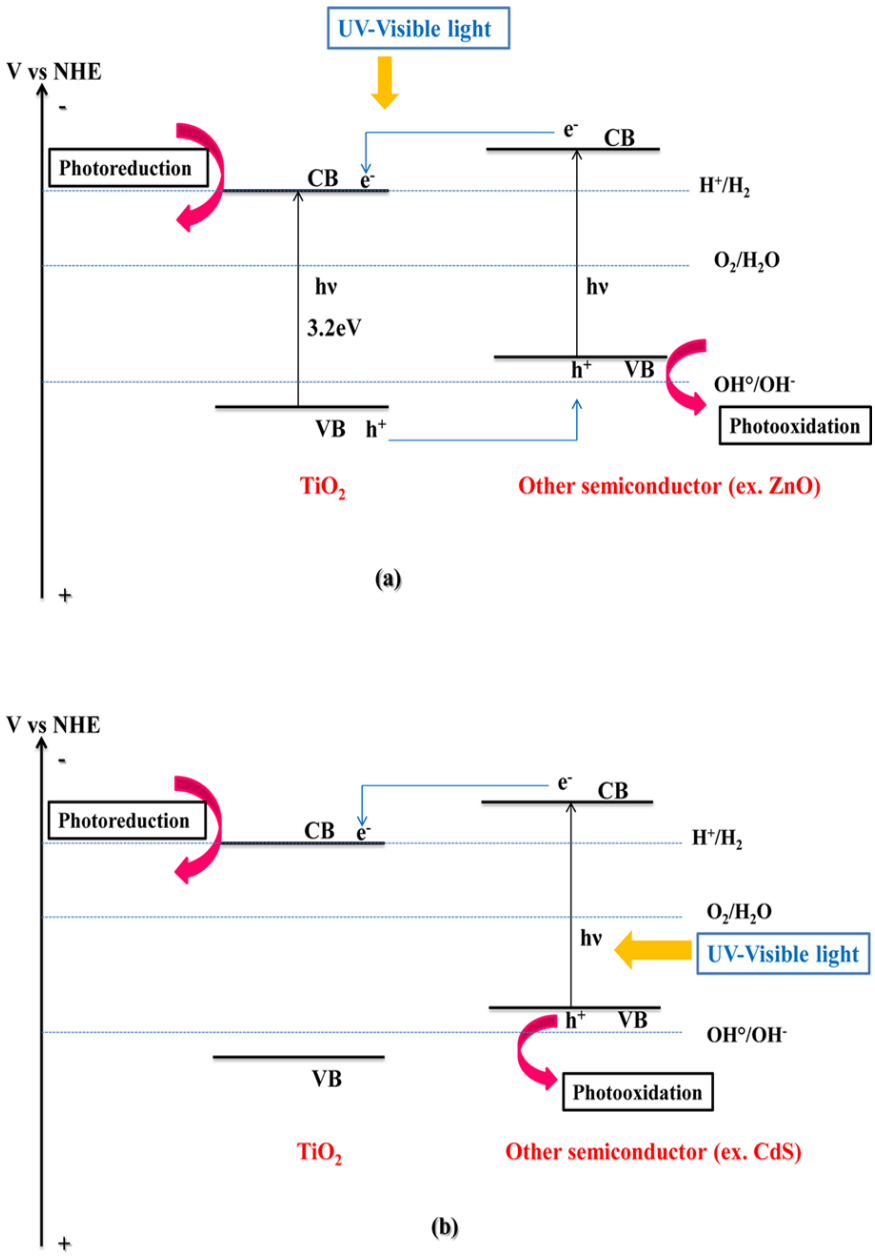

Figure 16: Vectorial transfer of electrons−holes in coupled semiconductor system:**(a)** when the conduction band of TiO_2 is more anodic than the corresponding band of the sensitizer and **(b)** when the valence band of the sensitizer is more cathodic than that of TiO_2 one [241].

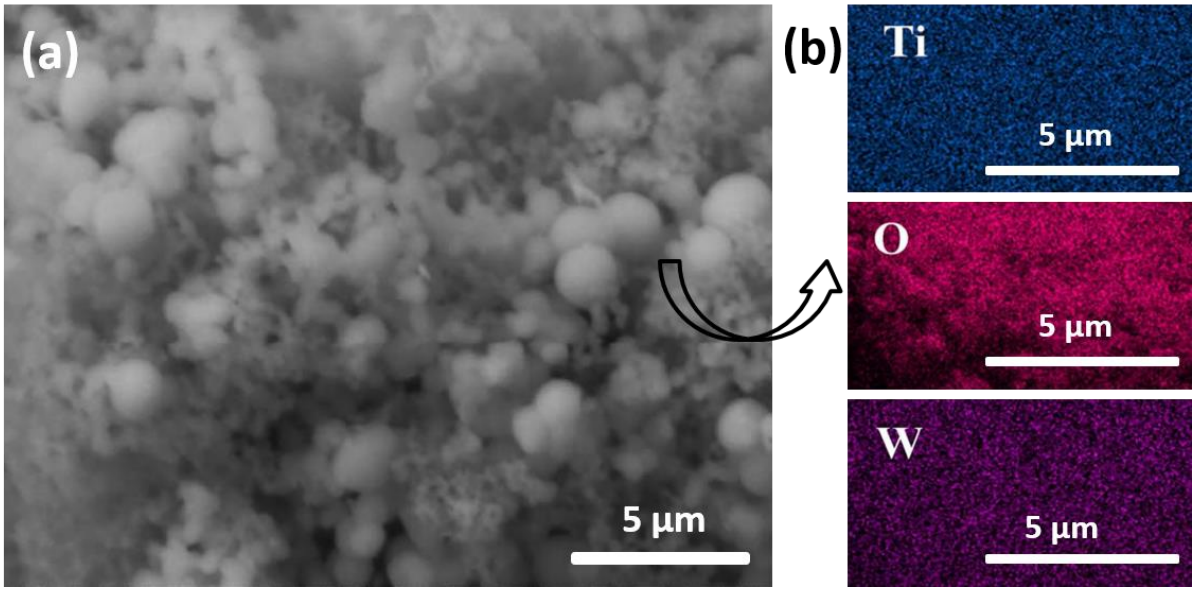

Figure 17: (a) SEM image and (b) EDX elemental mapping of TiO_2/WO_3 nanopowders, updated from reference [240].

5.5. Design of multiple components

The heterostructure junctions with built-in potential effectively drive the separation and transportation of photogenerated electron-hole pairs [242-245]. Different rational design and nanoscale integration of multiple components were elaborated in order to promote the photogenerated charge carriers and therefore improve the photocatalytic activity and stability [246,247]. A list of different multiple functional/TiO_2 based materials; their preparation methods and their photocatalytic applications are shown in Table 2. The reported studies show that the multiple functional components exhibit a higher photocatalytic performance compared to single - or two-component photocatalysts. For example, Sui *et al.*[33] fabricated Ag-AgBr/TiO_2 heterostructured nanofibers by combining solvothermal technique with photoreduction method. Ag-AgBr/TiO_2 heterostructured nanofibers showed an enhanced photocatalytic activity and good stability (reuse for up to five cycles) for the degradation of methylene blue under visible light compared with TiO_2 nanofibers and Ag-AgBr powder. These results were explained by the surface plasmon resonance effect of Ag nanoparticles and the synergetic effect between the three components of Ag, AgBr powder and TiO_2 nanofibers. Figure 18 shows the proposed photogenerated charge separation and migration process in Ag-AgBr/TiO_2 heterostructure. Hao *et al.* synthesized graphitic carbon nitride (g-

C_3N_4)/TiO_2 heterojunction photocatalysts by a facile calcination method. SEM image (Figure 19-a) shows that g-C_3N_4 particles were highly dispersed within the TiO_2 system. The g-C_3N_4 incorporation greatly improves the active surface area of g-C_3N_4/TiO_2 sample (70.2 m^2g^{-1}) compared with that of TiO_2 particles (34.8 m^2g^{-1}). Figure 19-b, represents the HRTEM image of g-C_3N_4/TiO_2 sample. The lattice fringes are clearly seen indicating the good crystallinity of anatase phase of TiO_2 with a lattice spacing of 0.35 nm corresponding to the (101) plane of TiO_2. The photocatalytic activity was tested by the degradation of rhodamine B under visible light. The enhanced photocatalytic activity was attributed to the high active surface area of g-C_3N_4/TiO_2 sample and to the close interfacial contact of the heterojunction which promote the transfer of photoinduced carriers from g-C_3N_4 to TiO_2 surface [248].

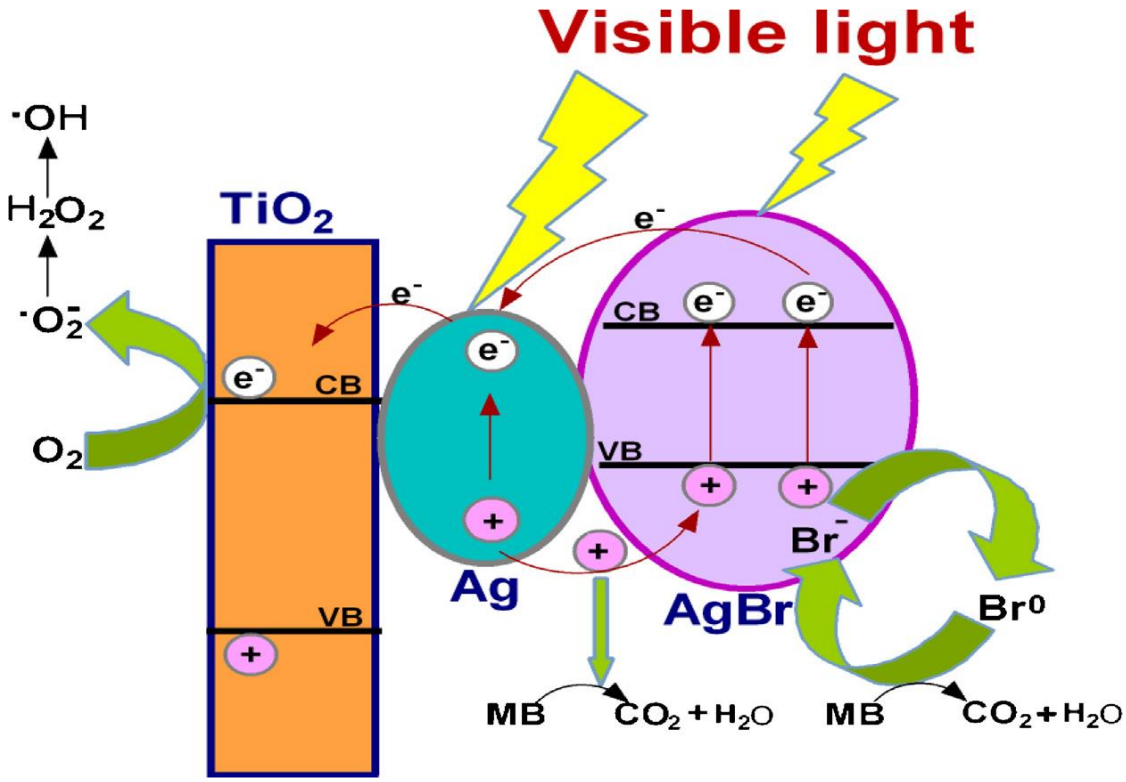

Figure 18: Proposed photogenerated charge separation and migration process in Ag AgBr/TiO_2 heterostructured nanofibers under visible light irradiation [33].

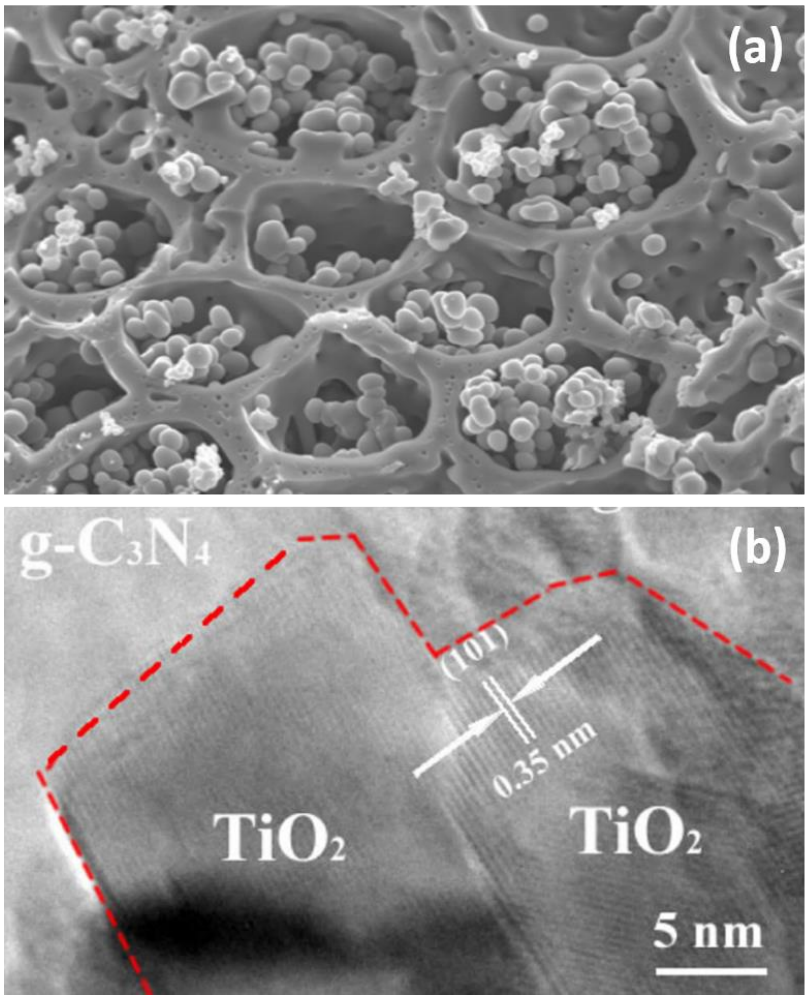

Figure 19: (a) SEM and (b) HRTEM images of g-C_3N_4/TiO_2 heterojunction photocatalyst [248].

Table 2: Different multiple functional/TiO_2 based materials, their preparation methods, their band gap, their photocatalysis application and their photocatalytic efficiency under visible light.

TiO_2 based heterostructures	**Preparation method**	**Band gap (ev)**	**Photocatalysis application**	**Photocatalytic efficiency**	**References**
Ag-AgBr/TiO_2 nanofibers	Solvothermal technique and photoreduction method	2.59	Degradation of methylen blue under visible light	2.5 times higher than TiO_2-P25	33
3D ordered assembly of Thin-Shell Au/TiO_2 hollow nanospheres	Layer-by-Layer technique	2.53	Decomposition of isopropanol	2.8 times higher than TiO_2-P25	249
Heterostructured g-C_3N_4(4%)/Ag/TiO_2 microspheres	Photodeposition method	2.68	Photodegradation of methyl orange	40 times higher than TiO_2 microspheres	250
Au-Pd/TiO_2 nanobelts	Deposition-	2.83	Aerobic oxidation	3 times higher	251

nanostructures	precipitation method		of benzyl alcohol	than Au/TiO_2 nanobelts	
Au–Cu nanoparticles supported on $SrTiO_3/TiO_2$ coaxial nanotube arrays	Hydrothermal and solvothermal methods	2.17	Photoreduction of CO_2 into CO	16 times higer than TiO_2 nanotube arrays	[252]
$CdS/Pt\text{-}TiO_2$ hybrids	Chemical precipitation	2.25	Hydrogen production	10 times higher than CdS/TiO_2	[253]
$Ag_3PO_4/TiO_2/Fe_3O_4$ heterostructure nanospheres	In situ hydrolysis and precipitation method.	2.75	Photodegradation of acid orange 7	5.1 times higher than TiO_2 nanoparticles	[254]
$Au/TiO_2–gC_3N_4$ nano-composites	Sol—gel and thermal polycondensation	2.45	Hydrogen production	1.5 times higher than Au/TiO_2 composites	[255]

The most efficient recent strategies to enhance the visible light photocatalytic activity of TiO_2 were discussed in this section. As results, there is a critical necessity to further develop these strategies with the purpose to be used in the industrial field. The TiO_2 based photocatalyst could be used in different photocatalytic applications in energy conversion and environmental remediation purposes as it will be discussed in the following section.

6. Photocatalytic applications

Increasing the need of clean water sources due to the rapid development of industries, population growth, science and technology have become issues worldwide. Recently, much attention was devoted to the photocatalysis process for water depollution. In addition, the photocatalysis process also concerns the energy storage via the ability to produce hydrogen and to photoreduce CO_2 into energy fuel. In this section, we will briefly discuss the implication of TiO_2 in the various photocatalytic applications for water sources treatment, hydrogen production, photodynamic therapy, photoelectric sensing and photocatalytic reduction of CO_2.

6.1. Pollutant degradation

Water pollution by some industrial, pharmaceutical and agricultural chemicals constitutes a source of environmental degradation and is currently attracting a particular

national and international attention [256]. Several types of organic and inorganic pollutants have been identified in industrial effluents such as dyes, heavy metals and pharmaceutical products[3,257,258]. The degradation of these pollutants by photocatalysis process will be discussed in this section.

6.1.1. Organic compounds

Because the textile industry uses large volume of water, a large number of organic compounds is released into the environment [259]. Organic pollutants are defined by the following properties: (1) toxicity: they have one or more harmful impacts on human health as well as on the environment [260]; (2) persistence in the environment: there are molecules that resist natural biological degradation; (3) bioaccumulation: the molecules accumulate in living tissues [261]. In addition to their properties of persistence and bioaccumulation, these molecules tend to move along very long distances and they deposit away from their emission sites, such as pesticides, hydrocarbons, dyes, drugs etc.[262-265]. Removing organic contaminants via photocatalysis has been shown to be more efficient than conventional waste water treatment such as filtration [266]. Several studies reported on the photodegradation of dyes as model pollutants by TiO_2-based photocatalyst under visible light include methylene blue[267], methyl orange[268], rodamine B[269-271], brilliant green [272,273], phenol [274,275] and acid red [276,277]. Wand *et al.*[278] elaborated carbon-sensitized and nitrogen-doped TiO_2 (C/N–TiO_2) using sol-gel method. They obtained a high efficient photodegradation of sulfanilamide (SNM) under visible light due to the incorporated carbon which serves as photosensitizer and the nitrogen doping which is responsible of the absorption edge red shift of C/N–TiO_2. Senthilnathan *et al.*[279] used lindane, an insecticide, as a target pollutant. They found that lindane was completely degraded under visible light by N-TiO_2 photocatalyst.

6.1.2. Heavy metals

Heavy metals are numerous and their toxicity depends on the context in which they are located and their concentration in aquatic environments [280]. In environmental science, heavy metals associated to the pollution and toxicity are generally cadmium (Cd), chromium (Cr), mercury (Hg), manganese (Mn), arsenic (As), nickel (Ni) and lead (Pb) [281]. When we discuss the problem of heavy metals, it is worth noting that these elements are found in our

everyday environment in different chemical forms which can confer a particular property (solubility, toxicity) on the studied metal [282]. Schrank *et al.*[283] evaluated the effect of pH and pollutants concentration on the kinetics of the reactions. They concluded that Cr(VI) reduction using TiO_2-P25 as photocatalyst was faster in acidic pH (pH = 2.5) compared to neutral pH. Recently, Sreekantan *et al.*[284] synthesized Cu-TiO_2 nanotubes using electrochemical anodization. The results showed that the removal of Pb(II) heavy metal by Cu-TiO_2 photocatalyst was up to 97% due to Cu^{2+} ions which play an important role in suppressing the recombination of charge carriers. In 2016, Zhang *et al.*[285] developed TiO_2-modified sewage sludge carbon (SS-carbon). They reported that the combination of the SS carbon with TiO_2 doubled the adsorption capacity of mercury on the SS carbon, and the photocatalytic removal rate was increased to 151 g/kg compared to 87 g/kg for SS carbon only. In addition, they concluded that Hg(II) removal increased with the increase of pH value.

6.2. Bacterial removal for water disinfection

Over the past 35 years, the use of TiO_2 photocatalysis for remediation of contaminated water has been extensively reported [286]. TiO_2-mediated disinfection has been studied for the first time by Matsunaga *et al.*[287] when they reported the destruction of three different bacterial species (E. coli, Lactobacillus, Acidophilus) using Pt-TiO_2 as photocatalyst. Due to its strong oxidizing power, non-toxicity and long-term photostability, photocatalytic disinfection is a promising process compared to the chlorination and UV disinfection methods [288]. In another study, Matsunaga *et al.*[289] found an E. coli inactivation of 99% in deionized water. They suggested that cell death was caused by the inhibition of its respiratory activity caused by the decrease in coenzyme A. They also reported that no cell wall destruction caused by the semiconductor was observed. Other studies demonstrated that the oxidative damage is initially due to oxidation of the cell wall, where the TiO_2 photocatalytic surface allows first contact with the intact cells. Then, the oxidative damage of the cytoplasmic membrane occurs. The photocatalytic action progressively increases the cell permeability and then allows the release of the intracellular content leading eventually to death. These authors also suggested that free particles of TiO_2 could also penetrate the membrane of damaged cells and attack intracellular components, which can accelerate the cell death [290]. Nadtochenkoa *et al.*[291] showed that trapping holes in TiO_2 by the cell wall is

more efficient than photogenerated electrons trapping, leading to a decrease in electron/hole recombination. Several authors have reported that cell wall modification by UV/TiO_2 is the main cause of bacterial inactivation[292-294].

6.3. Photodynamic therapy

Recently, nanomaterials with photocatalytic behavior are attracting much attention as promising candidates to develop new photodynamic therapy strategies [295]. The photodynamic therapy (PDT) is a treatment used to reduce the volume of a massive tumor. This technique is used to treat certain cancers (lung, head, skin and prostate). PDT is a treatment technique based on the use of photosensitizers (PS) molecules, which are non-cytotoxic in the dark, and will be activated by a light irradiation with an appropriate wavelength. The activation of the PS will induce photo-oxidation reactions and generation of highly cytotoxic species (O_2 and reactive oxygen species (ROS)), which will lead to the destruction of the target (tumor cells) [296,297]. TiO_2 doped with Pt or Zn have been successfully synthesized by Lopera *et al.* They found a red shift in the absorption spectrum after TiO_2 doping, which allowed the production of ROS when the system is irradiated with visible light. The application of the synthesized materials as photosensitizers in PDT was tested for the treatment of cutaneous leishmaniasis (neglected disease) under visible light. As results, the synthesized metal-doped TiO_2 nanomaterials with a photo-activation potential exhibited a high activity (EC_{50} = 18.2 µg/mL) for the treatment of cutaneous leishmaniasis through photodynamic therapy under visible light [20]. Another recent study reported on the reduced GO/TiO_2 composites as photosensitizer in PDT application. RGO/TiO_2 composites with different amounts of GO were elaborated via simple hydrothermal method. The photo-killing effect of RGO/TiO_2 composites on HepG2 cells was examined under visible light. They concluded that the optimal percentage of RGO/TiO_2 which lead to the highest photocatalytic activity was found to be 20%. After evaluating the toxic effect of RGO/TiO_2 using HepG2 cells (usually used to test the toxicity of chemicals and drugs), it was found that these composites are no-toxic without irradiation. In addition, photocatalytic RGO/TiO_2 composites killed the HepG2 cells by apoptosis pathway. Therefore, the synthesized material can be used as promising drug for photocatalytic killing cancer cells by photodynamic therapy [298].

6.4. Hydrogen generation

The production of hydrogen by photocatalysis is based on the decomposition of many organic species (alcohols, acids ...). The main objective of photocatalysis is to directly use water, or polluted effluents as a source of hydrogen [299]. The following three mechanisms are used for the hydrogen production:

-(1) Mechanism for the dehydrogenation of an alcohol: when the reagent used to produce hydrogen is a pure alcohol, the resulting photocatalytic reaction corresponds to the dehydrogenation of this alcohol [300]. Higashimoto *et al.*[301] reported on the synthesis of CdS/TiO_2 photocatalyst modified with a Pd co-catalyst for the selective dehydrogenation of benzyl alcohol to benzaldehyde with high selectivity (>99%) accompanied by the formation of H_2 in aqueous solution under visible-light irradiation.

(2) Water splitting: this mechanism is one of the most attractive reactions for hydrogen production [91,302]. The objective is to use solar energy to obtain hydrogen from water, and then to use this hydrogen directly to produce electricity *via* a fuel cell. The chosen photocatalyst should have a conduction band with an electrochemical potential lower than that of the H^+/H_2 redox couple to reduce the hydrogen. In addition, the electrochemical potential of the photocatalyst's valence band should be greater than that of the O_2/H_2O redox couple to oxidize the water [303]. The photocatalytic hydrogen production by TiO_2 is shown in Figure 20. Thus, all the photocatalysts that satisfy the above-mentioned requirements are capable to reduce hydrogen or to oxidize water. TiO_2[304], $SrTiO_3$[305], $KTaO_3$ [306,307] and CdS [308,309] are the most used candidates for water splitting.

(3) Mechanism of an alcohol reforming: photocatalytic reforming of organic compounds such as alcohols is another method of hydrogen production. These reactions generally consist of several successive steps leading to the formation of CO_2 and H_2. Various alcohols have been used in this type of photocatalytic reforming reaction such as methanol, and ethanol [310,311]. The hydrogen produced by photocatalysis is not pure. The species present in the gas phase will be dependent on the organic compounds used for reforming. Thus, hydrogen is accompanied by different species such as CO_2, alkanes and aldehydes [312]. Recently, Kennedy *et al.*[313] produced hydrogen by methanol reforming using $Au\text{-}Ag/TiO_2$ photocatalyst prepared *via* sol immobilization. They studied the effect of gold loading over Au/TiO_2 catalysts. They showed that the maximum rate of H_2 production was observed for

Au loadings of 1–2 wt. %. In addition, they reported that the order of the metal addition is important for the preparation of active Au–Ag/TiO_2 photocatalysts and for the improvement of the hydrogen production.

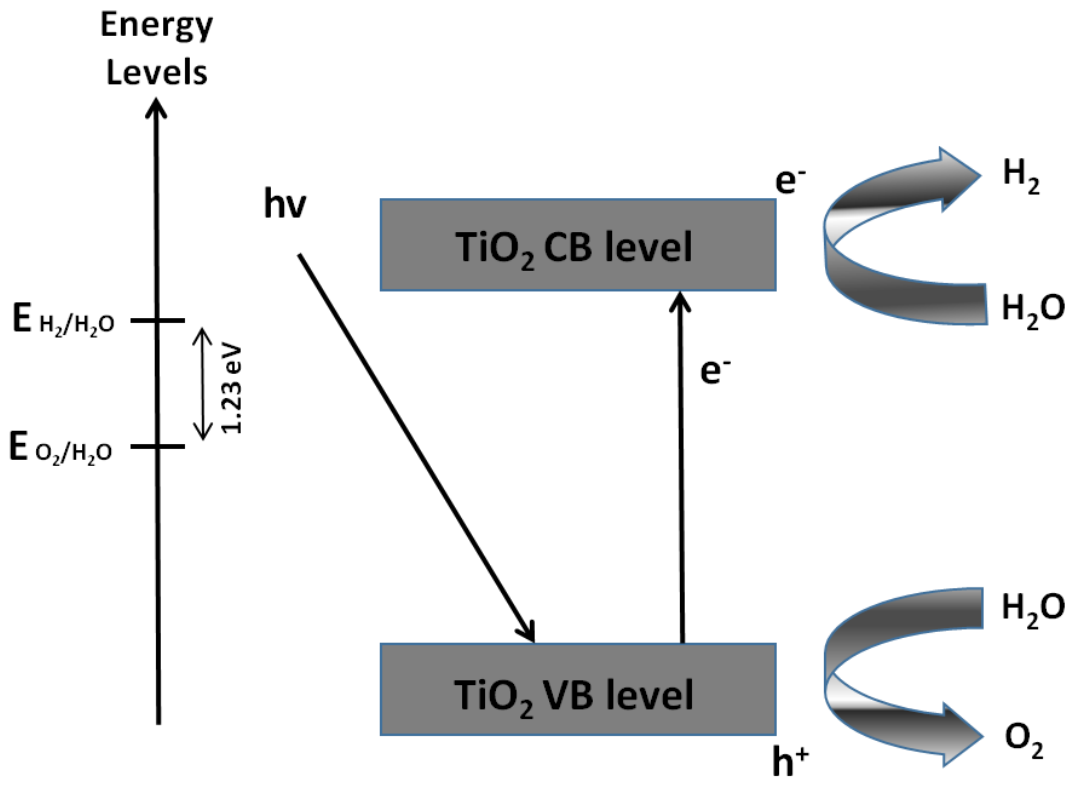

Figure 20: Mechanism of TiO_2 photocatalytic water-splitting for hydrogen production, updated from reference [302].

6.5. Photocatalytic reduction of CO_2

Recently, the increasing of fossil fuels consumption has caused a high CO_2 concentration in the atmosphere which leads to serious environmental pollution and global energy crisis. With the aim of reducing CO_2 concentration in the atmosphere, much attention has been devoted to the photocatalytic reduction of carbon dioxide into energy fuel [314,315]. These reactions imitate the natural photosynthesis by using photocatalyst materials to achieve the photoreduction of CO_2 into valuable solar fuels including methane, formic acid, formaldehyde and methanol[316]. Titanium dioxide, the most efficient photocatalyst, has been successfully used for the photocatalytic CO_2 reduction [21]. Figure 21 shows the mechanism of the photocatalytic CO_2 reduction when TiO_2 is applied as

photocatalyst. The absorption of sufficient photon energy will lead to electron-hole pair generation. The electron-hole pairs will migrate separately to the TiO_2 surface and reduce the adsorbed CO_2. Recently, Lei *et al.*[317] reported a one-step solvothermal method to synthesize carbon nanofibers (CNFs) supported TiO_2 nanocrystals (NCs) with {001} and {101} facets co-exposure (CNF-001/101TiO_2). Three samples with different mass ratios of CNF/TiO_2 (1%, 5% and 10% corresponding to 1CNF-001/101TiO_2, 5CNF-001/101TiO_2 and 10CNF-001/101TiO_2, respectively) were elaborated. The CO_2 photocatalytic reduction into CO was investigated under simulated sunlight. It was found that 5CNF-001/101TiO_2 sample exhibits the highest CO amount (2.4 $\mu molg^{-1}$) compared with other samples. The enhanced photocatalytic CO_2 reduction was attributed to the efficient separation of photogenerated charges due to the formation of {001}/{101} surface heterojunction within TiO_2 crystals and TiO_2-carbon heterojunction between TiO_2 and carbon nanofibers [317]. Moreover, Jiang *et al.*[318] proposed to use Ag noble metal and activated carbon to modify the properties of TiO_2 and improve its photocatalytic CO_2 reduction. TiO_2/AC-Ag composite photocatalyst was prepared by ultra-sonication and photo-deposition methods. They found that TiO_2/AC-Ag has a large specific surface area and consequently a high CO_2 adsorption capacity which is in favor of CO_2 photoconversion efficiency compared with pure TiO_2. In addition, the effective charge separation was attributed to the good electrical conductivity of the activated carbon. Due to the surface plasmon resonance of Ag, the photocatalyst was able to absorb light in a broader spectrum. As results, the CO_2 photoreduction into CO of TiO_2/AC-Ag (3.62 $\mu molg^{-1}$) was 6 times higher than that of pure TiO_2 (0.59$\mu molg^{-1}$)[318].

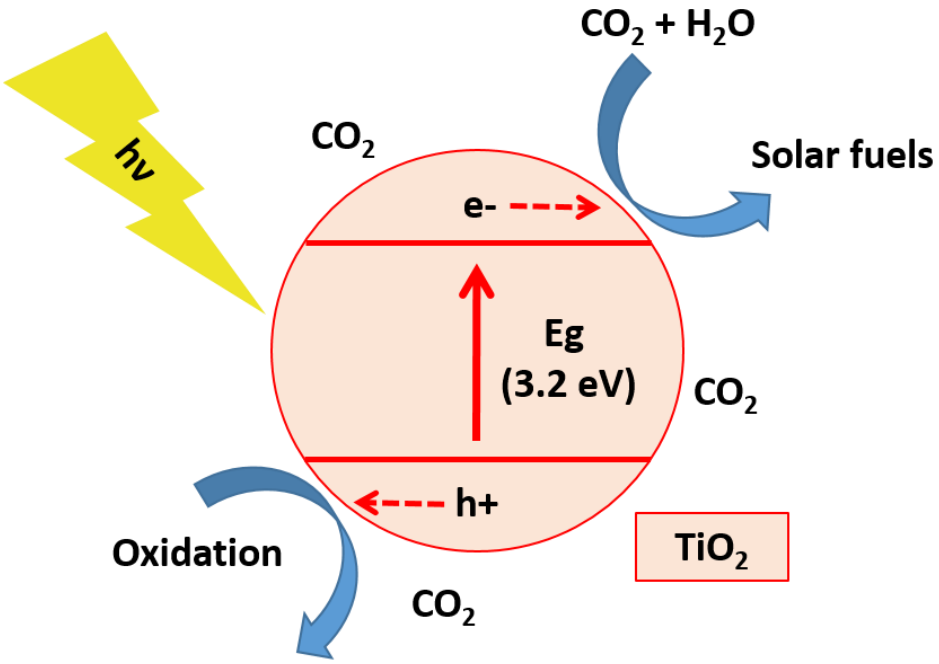

Figure 21: Schematic illustration of the photocatalytic CO_2 reduction mechanism on the TiO_2 surface.

6.6. Photoelectric sensing

Several oxides have been used for photoelectric sensing including ZnO, TiO_2, SnO_2, WO_3 [319]. Among these oxides, TiO_2 showed enormous potential in the field of photoelectric sensing. It was employed to detect the presence of different gases in a specific area [320]. Recently, Wu *et al.*[321] have significantly improved the visible light photo-response of a single TiO_2 nanowire by nitrogen ion implantation and they applied the N-doped single TiO_2 nanowire to visible light detection for the first time. It was found that under high electric field (bias voltage 3V) and under the same intensity of light illumination, the photoelectric properties were improved, therefore, more charge carries are excited. Thus, with a higher bias voltage, it is more difficult for the electron hole pairs to recombine. As results, the elaborated photodetector based on single N-TiO_2 nanowire exhibits excellent performance in visible light detection, the responsivity reached 300 AW^{-1} under a bias voltage of 3 V[321]. In order to evaluate the photoelectric gas sensing properties, Zou *et al.*[322] have fabricated a flat-type device based on CdS/TiO_2 nanocomposite films. They used the screen printing method to design the Au interdigital electrodes on alumina substrate. Formaldehyde has been used as a model pollutant to evaluate the photoelectric gas sensing of pure TiO_2 and

CdS/TiO_2 nanocomposite devices under visible light. With the aim to promote the charge separation, different bias voltages were applied. As results, they concluded that CdS/TiO_2 nanocomposite device exhibit an obvious enhancement of photocurrent response compared with pure TiO_2. In fact, CdS works as a sensitizer and makes the CdS/TiO_2 device sensitive to the visible light, while TiO_2 represents the gas sensing units and the photo-generated electron's acceptors [322].

Table 3 summarized the most current TiO_2 nanostructures based material, their preparation methods, their band gap, their photocatalytic efficiency and their photocatalytic applications. The reported studies show the great progress achieved with several TiO_2 nanostructures for different photocatalytic applications, however it is worth noting that much attention were devoted to the water purification and disinfection compared to other photocatalytic applications[323]. Now, it is well-established that energy production and environmental challenges constitute issues worldwide. Therefore, we can assume that the TiO_2 photocatalysis applications should have a future beneficial impact on the environment, energy production and public health. In addition, the results found so far are still limited to the laboratory scale. Further researchers should be performed in order to use photocatalysis on a larger scale in commercial and industrial processes.

Table 3. Summary of recent studies on TiO_2 based material, nanostructures, preparation methods, band gap, photocatalytic efficiency and photocatalysis application.

TiO_2 based material	**Nanostructure**	**Synthesis technique**	**Band gap (eV)**	**Photocatalytic efficiency**	**Photocatalytic application**	**Ref**
BN-Ag/TiO_2	Nanofibers	Electrospinning	2.80	98%	Degradation of MB	144
g-C_3N_4/TiO_2	TiO_2 spheres wrapped with lamellar g-C_3N_4	Hydrothermal	2.48	Total removal of 10^7 cfu.ml^{-1}	Inactivation of *E. coli*	324
AgI/TiO_2	nanoparticles	Dissolution-precipitation	2.67	96%	Reduction of Cromium (VI)	325
rGO-TiO_2	Nanofibers	Electrospinning	2.95	90%	Degradation of MO	70
Pt-doped TiO_2	Hollow spheres	Sol-gel	–	1023.71 µmol h^{-1} g^{-1}	Hydrogen production	326
rGO-TiO_2	Nanoparticles	Hydrothermal	–	Total removal	Removal of antibiotics	327
FeS_2/TiO_2	Nanotubes	Anodic oxidation & Hydrothermal	1.70	91.7 µmol h^{-1} L^{-1}	Reduction of CO_2 into methanol	328

$ZnFe_2O_4$@TiO_2	Nanofibers	Electrospinning & PECVD	2.78	98%	Degradation of MB	[329]
Pt doped TiO_2	Nanoparticles	Solution-combustion	3.01	EC_{50} = 18.2 µg/mL	PDT (antileishmanial activity)	[20]
N-doped TiO_2	Nanoparticles	Sol-gel	2.50	52%	Degradation of EBT	[330]
Ag-NPs/TiO_2 NWs	Core/shell heterojunction	Photo-deposition	3.16	983 µmole g-catal^{-1}h^{-1}	Reduction of CO_2 into CO	[331]
CdS@TiO_2	Core-Shell Nanorods	Sol-gel	2.45	80%	Degradation of phenol	[332]
TiO_2/CuS	Core-Shell Nanorods	Hydrothermal & Solvohermal	2.62	90%	Degradation of MB	[333]
Graphene-sensitized TiO_2	Graphene quantum dots-TiO_2 nanotubes	Electrochemical anodization	-	1.98 ppm cm^{-2} h^{-1}	Reduction of CO_2 into CH_4	[334]
TiO_2 coated alumina	Nanowires	Template approach	3.2	90%	Degradation of MB	[335]
rGO-TiO_2	Nanoparticles	Hydrothermal	-	Total removal	PDT (Photokilling of HepG2 cells)	[298]

7. Scale up and Commercialization

Despite that the laboratory studies have proven a strong potential of the photocatalytic process, commercial applications (large scale) have been late to come out for several reasons. Firstly, the use of titanium dioxide as powder requires a filtration step, which is considered as an expensive treatment. Therefore, TiO_2 in powder form was replaced by supported catalysts. The main reason remains the lack of regulation on limited volumes of polluted water. Different configurations for solar TiO_2 photocatalytic reactors have been designed to be used for large scale applications such as parabolic trough, flat plate, open tank, double skin sheet and shallow ponds [336].The pioneers in this field are the American laboratories and “Plataforma Solar de Almería (PSA) of CIEMAT”, Spain. The same depollution reactions studied at the laboratory scale have been successfully transposed on a pilot scale at the solar platform of Almeria using a parabolic trough reactor under the 3 to 5% of UV-A light from the solar spectrum [337]. With the aim of producing about 1 m^3 of drinking water per day by solar photocatalysis, two European programs, "Solwater" with Latin America and "Aquacat" with North Africa have made it possible [338]. As shown in Figure 22, they developed an autonomous solar prototype to provide clean drinking water for the

communities without clean water or electricity in semi-arid regions, where solar irradiance is considerable, including Egypt, Tunisia, Morocco, Peru, Mexico and Argentina. Recently, in 2013, a pilot plant study was carried out by Hendarsa *et al.* in Grati, East Java, Indonesia. They used an open tank reactor to treat 4000 liters of hydrocarbon wastewater. They obtained an average removal rates of 98% for ammonia and phenol [339]. Recent pilot studies have been focused on the TiO_2 photocatalysis using the UV light from solar spectrum, therefore future environmental research programs should be devoted to scale up by producing more pilot studies using the visible light from solar spectrum.

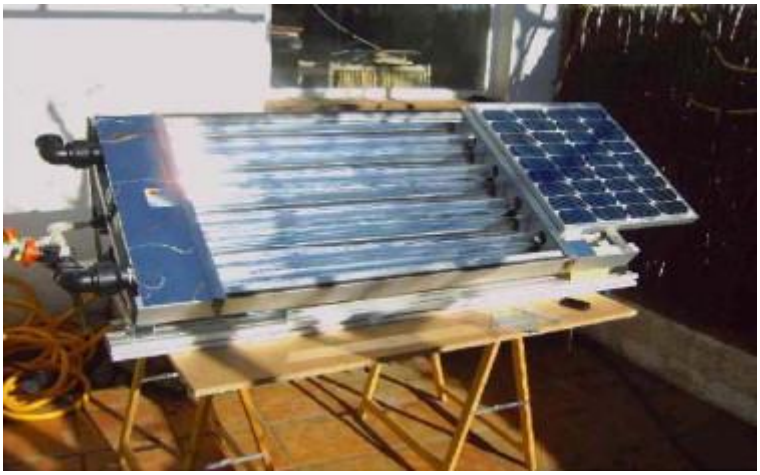

Figure 22: Autonomous solar prototype of water purification of European projects AQUACAT and SOLWATER [338].

8. Conclusion and Perspectives

Since the two principle limitations of TiO_2 are the fast charge recombination and the UV absorption edge, many efforts have been devoted to develop a new TiO_2 photocatalyst with low charge recombination rate and able to absorb visible light which is the main part of solar spectrum. The present review has summarized the recent research development to enhance the photocatalytic activity of TiO_2 photocatalyst under visible light and solar irradiation. First, we introduced current techniques used to synthesize 0D, 1D and 2D nanostructures of TiO_2 based materials including solvothermal, electro-deposition, electrospinning, hydrothermal, electrochemical anodization, template assisted method, sol-gel, spin coating, dip coating, chemical vapor deposition and atomic layer deposition, as we defined the advantages and limitations of each technique and we showed the impact of the TiO_2 morphology on the photocatalytic activity. Till now, the development of novel TiO_2

based material designs remains a big interest for future studies. In the second section of this review, we studied the effect of the operating parameters (the pH of the solution, the initial concentration of the organic compound, the catalyst concentration, the oxygen content and the temperature) on the photocatalytic process. In order to promote the charge separation efficiency and to improve the visible light photocatalytic activity of TiO_2, different strategies were discussed such as metal doping, surface modification with metal elements, modification with non-metal elements, coupling of two semiconductors, metal deposition on the surface of TiO_2 and design of multiple components. These strategies promote the charge separation of TiO_2 and extend the absorption to the visible region allowing the use of solar light to achieve the photocatalytic process. Despite the achieved high photocatalytic efficiency using these laboratory strategies, it is clear that they are not competent for scale-up and commercialization. Thus, more effort should be devoted on the development of new efficient strategies to increase the efficiency of visible light photocatalytic activity of TiO_2 for large scale application. Photocatalytic process can be used for several applications including the treatment of wastewater for the removal of heavy metals and organic compounds, water disinfection, hydrogen production, photodynamic therapy, photoelectric sensing and photocatalytic reduction of CO_2. Therefore, we summarized in this review, the greatest achieved works for each application. Also, we highlighted the recent progress produced on TiO_2 photocatalysis for large scale applications. In summary, despite the great achievement and the development in the past decades, the possibility of TiO_2 modification for more efficient photocatalytic applications apparently has not been fully explored. Future researches should be focused on the development of new strategies to improve the properties and the photocatalytic efficiency of TiO_2 nanomaterials. We hopefully believed that this comprehensive review will help future research to provide new insights in exploring new strategies with the aim of enhancing the photocatalytic efficiency of TiO_2 in the visible light range.

References

1. Hoffmann, M. R*., et al.*, *Chemical reviews* (1995) **95** (1), 69
2. Zhai, C*., et al.*, *Physical Chemistry Chemical Physics* (2014) **16** (28), 14800
3. Nasr, M*., et al.*, *Superlattices and Microstructures* (2015) **77**, 18

4. Dąbrowski, A.*, et al.*, *Chemosphere* (2004) **56** (2), 91
5. Legrini, O.*, et al.*, *Chemical reviews* (1993) **93** (2), 671
6. Ganiyu, S. O.*, et al.*, *Journal of Materials Chemistry A* (2017) **5** (7), 3655
7. Le, T. X. H.*, et al.*, *Journal of Materials Chemistry A* (2016) **4** (45), 17686
8. Ali, I., and Gupta, V., *Nature protocols* (2006) **1** (6), 2661
9. Pokhrel, D., and Viraraghavan, T., *Science of the total environment* (2004) **333** (1), 37
10. Xu, X.*, et al.*, *Journal of Materials Chemistry A* (2014) **2** (1), 116
11. Kannan, N., and Sundaram, M. M., *Dyes and pigments* (2001) **51** (1), 25
12. Jiang, L.*, et al.*, *Journal of colloid and interface science* (2015) **439**, 62
13. Jiang, Z.*, et al.*, *Energy & Environmental Science* (2018)
14. Sofianou, M.-V.*, et al.*, *Applied Catalysis B: Environmental* (2015) **162**, 27
15. Le, T. X. H.*, et al.*, *RSC Advances* (2015) **5** (53), 42536
16. Serpone, N., and Pelizzetti, E., (1989)
17. Low, J.*, et al.*, *Applied Surface Science* (2017) **392**, 658
18. Wang, Q.*, et al.*, *Nanoscale* (2017) **9** (46), 18194
19. Zhang, C.*, et al.*, *ACS applied materials & interfaces* (2017)
20. Lopera, A.*, et al.*, *Journal of Photochemistry and Photobiology B: Biology* (2018) **183**, 64
21. Luo, D.*, et al.*, CO2 Reduction by Photocatalysis on TiO2. In *Advanced Solid Catalysts for Renewable Energy Production*, IGI Global(2018), pp 268
22. Patil, S.*, et al.*, *Journal of Physics and Chemistry of Solids* (2018) **115**, 127
23. Linsebigler, A. L.*, et al.*, *Chemical reviews* (1995) **95** (3), 735
24. Fujishima, A., and Honda, K., *nature* (1972) **238** (5358), 37
25. Konstantinou, I. K., and Albanis, T. A., *Applied Catalysis B: Environmental* (2004) **49** (1), 1
26. Liang, P.*, et al.*, *Micro & Nano Letters* (2016) **11** (9), 539
27. Nasr, M.*, et al.*, *New Journal of Chemistry* (2017) **41** (1), 81
28. Reddy, K. R.*, et al.*, *Applied Catalysis A: General* (2015) **489**, 1
29. Ye, J.*, et al.*, *Journal of the American Chemical Society* (2010) **133** (4), 933
30. Braun, J. H., *JCT, Journal of coatings technology* (1997) **69** (868), 59
31. Van der Meulen, T.*, et al.*, *Journal of Catalysis* (2007) **251** (1), 131
32. Yang, D.*, et al.*, *The Journal of Physical Chemistry C* (2015) **119** (11), 5827
33. Sui, Y.*, et al.*, *Journal of Molecular Catalysis A: Chemical* (2015) **410**, 226
34. Wang, M.*, et al.*, *Journal of Materials Chemistry A* (2016) **4** (19), 7190
35. Ide, Y.*, et al.*, *Physical Chemistry Chemical Physics* (2015) **18** (1), 79
36. Wei, Z.*, et al.*, *Separation and Purification Technology* (2014) **122**, 60
37. Farner Budarz, J.*, et al.*, *Langmuir* (2017) **33** (11), 2770
38. Thomas, M., and Natarajan, T. S., *Photocatalytic Nanomaterials for Environmental Applications* (2018) **27**, 48
39. Ge, M.*, et al.*, *International Journal of Hydrogen Energy* (2017) **42** (12), 8418
40. Hadnadjev-Kostic, M.*, et al.*, *Journal of Cleaner Production* (2017) **164**, 1
41. Bhanvase, B.*, et al.*, *Environmental Technology Reviews* (2017) **6** (1), 1
42. Wang, M.*, et al.*, *Energy & Environmental Science* (2014) **7** (7), 2182
43. Hashimoto, K.*, et al.*, *Japanese journal of applied physics* (2005) **44** (12R), 8269
44. Testino, A.*, et al.*, *Journal of the American Chemical Society* (2007) **129** (12), 3564
45. Nakade, S.*, et al.*, *The Journal of Physical Chemistry B* (2002) **106** (39), 10004
46. Wang, P.*, et al.*, *The Journal of Physical Chemistry B* (2003) **107** (51), 14336
47. Atyaoui, A., Elaboration de TiO2 sous forme de couche mince dopée et nanotubulaire: caractérisation électrochimique et performance photocatalytique. Université Pierre et Marie Curie-Paris VI2013
48. Ramakrishnan, V. M.*, et al.*, *Materials Research Bulletin* (2018) **97**, 351

49. Navab, A. A.*, et al.*, Hydrothermal synthesis of TiO2 nanorod for using as an electron transport material in perovskite solar cells. In *AIP Conference Proceedings*, AIP Publishing(2018), Vol. 1920, p 020015
50. Shu, W.*, et al.*, *Journal of Alloys and Compounds* (2013) **563**, 229
51. Li, X. L.*, et al.*, *Chemistry-A European Journal* (2006) **12** (8), 2383
52. Bhorde, A.*, et al.*, *Applied Physics A* (2018) **124** (2), 133
53. Liu, X.*, et al.*, *Applied Catalysis A: General* (2018) **550**, 11
54. Mihankhah, T.*, et al.*, *International Journal of Green Energy* (2018), 1
55. Vanrenterghem, B.*, et al.*, *Applied Catalysis B: Environmental* (2018)
56. Endrődi, B.*, et al.*, *ACS Applied Energy Materials* (2018)
57. Dong, K.*, et al.*, *RSC Advances* (2017) **7** (27), 16535
58. Low, J.*, et al.*, *Applied Surface Science* (2018) **434**, 423
59. Kim, H.*, et al.*, *Precision Engineering* (2018) **51**, 153
60. Zhu, J.*, et al.*, *Journal of Molecular Catalysis A: Chemical* (2004) **216** (1), 35
61. Ruiz, A. M.*, et al.*, *Sensors and Actuators B: Chemical* (2005) **109** (1), 7
62. Ho, W.*, et al.*, *Journal of solid state chemistry* (2006) **179** (4), 1171
63. MacDiarmid, A.*, et al.*, *Synthetic Metals* (2001) **119** (1-3), 27
64. Doshi, J., and Reneker, D. H., Electrospinning process and applications of electrospun fibers. In *Industry Applications Society Annual Meeting, 1993., Conference Record of the 1993 IEEE*, IEEE(1993), pp 1698
65. Chronakis, I. S., *Journal of materials processing technology* (2005) **167** (2), 283
66. Yarin, A. L.*, et al.*, *Journal of applied physics* (2001) **90** (9), 4836
67. Baji, A.*, et al.*, *Composites science and technology* (2010) **70** (5), 703
68. Casper, C. L.*, et al.*, *Macromolecules* (2004) **37** (2), 573
69. Onozuka, K.*, et al.*, *Nanotechnology* (2006) **17** (4), 1026
70. Nasr, M.*, et al.*, *The Journal of Physical Chemistry C* (2016) **121** (1), 261
71. Zhang, X.*, et al.*, *The Journal of Physical Chemistry C* (2012) **116** (28), 14780
72. Shahgaldi, S.*, et al.*, *International Journal of Hydrogen Energy* (2012) **37** (15), 11237
73. Park, J. Y.*, et al.*, *Journal of the American Ceramic Society* (2009) **92** (11), 2551
74. Yousef, A.*, et al.*, *Ceramics International* (2012) **38** (6), 4525
75. Nalbandian, M. J.*, et al.*, *Journal of hazardous materials* (2015) **299**, 141
76. Yanagisawa, K., and Ovenstone, J., *The Journal of Physical Chemistry B* (1999) **103** (37), 7781
77. Ismail, A. A.*, et al.*, *Materials Letters* (2005) **59** (14), 1924
78. Xu, Y.*, et al.*, *ACS nano* (2010) **4** (7), 4324
79. Akhtar, J., and Amin, N. A. S., *Renewable and Sustainable Energy Reviews* (2011) **15** (3), 1615
80. Tian, J.*, et al.*, *Chemical Society Reviews* (2014) **43** (20), 6920
81. Bavykin, D. V.*, et al.*, *Chemical Communications* (2013) **49** (62), 7007
82. Venkatachalam, S.*, et al.*, Preparation and characterization of nanostructured TiO2 thin films by hydrothermal and anodization methods. In *Optoelectronics-Advanced Materials and Devices*, InTech(2013)
83. Sheng, X.*, et al.*, *Chemical Science* (2016) **7** (3), 1910
84. Mao, M.*, et al.*, *Nanoscale* (2014) **6** (21), 12350
85. Liu, Z.*, et al.*, *Environmental science & technology* (2008) **42** (22), 8547
86. Li, J.*, et al.*, *Materials Chemistry and Physics* (2017) **190**, 202
87. Lee, C. H.*, et al.*, *Molecular Crystals and Liquid Crystals* (2011) **539** (1), 125/[465]
88. Kmentova, H.*, et al.*, *Catalysis Today* (2017) **287**, 130
89. Macak, J. M.*, et al.*, *Current Opinion in Solid State and Materials Science* (2007) **11** (1-2), 3
90. Ye, Y.*, et al.*, *Applied Catalysis B: Environmental* (2018) **220**, 171
91. Ge, M.*, et al.*, *Advanced Science* (2017) **4** (1)
92. Taziwa, R.*, et al.*, *J Nanosci Nanotechnol Res* (2017) **1** (1), 4
93. Lee, J.*, et al.*, *Sensors and Actuators B: Chemical* (2011) **160** (1), 1494

94. Lee, J.-H.*, et al.*, *The Journal of Physical Chemistry B* (2005) **109** (27), 13056
95. Pang, Y.*, et al.*, *Applied Surface Science* (2017) **420**, 361
96. Li, Y.*, et al.*, *Carbon* (2017) **122**, 237
97. Lee, H.-G.*, et al.*, *Journal of hazardous materials* (2015) **283**, 400
98. Procopio, E. Q.*, et al.*, *Nanotechnology* (2018) **29** (5), 055704
99. Nocuń, M.*, et al.*, *Journal of Molecular Structure* (2018) **1167**, 194
100. López-Ramón, M. V.*, et al.*, *Journal of colloid and interface science* (2018) **511**, 193
101. Tabesh, S.*, et al.*, *Journal of Alloys and Compounds* (2018) **730**, 441
102. Wellia, D. V.*, et al.*, *Indonesian Journal of Pure and Applied Chemistry Research* (2018) **7** (1)
103. Khore, S. K.*, et al.*, *RSC Advances* (2017) **7** (52), 33029
104. Macwan, D.*, et al.*, *Journal of materials science* (2011) **46** (11), 3669
105. Sahu, N.*, et al.*, *Indian Journal of Physics* (2009) **83** (4), 493
106. Krebs, F. C., *Solar energy materials and solar cells* (2009) **93** (4), 394
107. Hall, D. B.*, et al.*, *Polymer Engineering & Science* (1998) **38** (12), 2039
108. Pan, J. H., and Lee, W. I., *Chemistry of Materials* (2006) **18** (3), 847
109. Darwish, A.*, et al.*, *International Journal of Nanoscience* (2017) **16** (02), 1650028
110. Lourduraj, S., and Williams, R. V., *Journal of Advanced Dielectrics* (2017) **7** (04), 1750024
111. Brinker, C.*, et al.*, *Thin solid films* (1991) **201** (1), 97
112. Strawbridge, I., and James, P., *Journal of non-crystalline solids* (1986) **86** (3), 381
113. Grosso, D., *Journal of Materials Chemistry* (2011) **21** (43), 17033
114. Nishio, K.*, et al.*, *Journal of materials science* (1996) **31** (7), 1761
115. Nandi, B.*, et al.*, *Journal of Membrane Science* (2009) **330** (1), 246
116. Janczarek, M.*, et al.*, *Photochemical & Photobiological Sciences* (2015) **14** (3), 591
117. Roy, S.*, et al.*, *Applied Surface Science* (2018)
118. Falk, G.*, et al.*, *Journal of Nanoparticle Research* (2018) **20** (2), 23
119. Chayahara, A.*, et al.*, *Japanese journal of applied physics* (1987) **26** (9A), L1435
120. Lin, Y., and Burggraaf, A., *AIChE journal* (1992) **38** (3), 445
121. Piccirillo, C.*, et al.*, *Chemical Vapor Deposition* (2007) **13** (4), 145
122. Hess, D. W., *Journal of Vacuum Science & Technology A: Vacuum, Surfaces, and Films* (1984) **2** (2), 244
123. Quesada-Cabrera, R.*, et al.*, *Journal of Photochemistry and Photobiology A: Chemistry* (2017) **333**, 49
124. Yoshitake, H.*, et al.*, *Chemistry of Materials* (2002) **14** (3), 1023
125. Youssef, L.*, et al.*, *Journal of the European Ceramic Society* (2017)
126. Hass, G.*, et al.*, *Physics of Thin Films: Advances in Research and Development*. Elsevier: 2013
127. Chaaya, A. A.*, et al.*, *Beilstein journal of nanotechnology* (2013) **4** (1), 690
128. Cabello-Aguilar, S.*, et al.*, *Nanoscale* (2013) **5** (20), 9582
129. Jedrzejewska-Szczerska, M.*, et al.*, *Sens. Actuator A-Phys.* (2015) **221**, 88
130. Weber, M.*, et al.*, *ACS applied materials & interfaces* (2017) **9** (19), 16669
131. Baitimirova, M.*, et al.*, *J. Phys. Chem. C* (2016) **120** (41), 23716
132. Viter, R.*, et al.*, *Nanotechnology* (2015) **26** (10)
133. Abou Chaaya, A.*, et al.*, *J. Phys. Chem. C* (2013) **117** (29), 15306
134. Sveshnikova, G.*, et al.*, *J. Appl. Chem. USSR* (1967) **40**, 2644
135. Johnson, R. W.*, et al.*, *Materials today* (2014) **17** (5), 236
136. Puurunen, R. L., *Journal of applied physics* (2005) **97** (12), 9
137. George, S. M., *Chem. Rev* (2010) **110** (1), 111
138. Pinna, N., and Knez, M., *Atomic layer deposition of nanostructured materials*. John Wiley & Sons: 2012
139. K Patil, M.*, et al.*, *Current Nanoscience* (2015) **11** (3), 271
140. Yang, Y.*, et al.*, *ACS nano* (2009) **3** (3), 555
141. Kayaci, F.*, et al.*, *Nanoscale* (2014) **6** (11), 5735

142. Chen, Q*., et al.*, *Journal of Materials Science: Materials in Electronics* (2017) **28** (4), 3865
143. Zhou, Y*., et al.*, *Applied Catalysis B: Environmental* (2010) **101** (1), 54
144. Nasr, M*., et al.*, *New Journal of Chemistry* (2018)
145. Nasr, M*., et al.*, *RSC Advances* (2016) **6** (105), 103692
146. Nasr, M*., et al.*, *Surface and Coatings Technology* (2017)
147. Ahmed, S*., et al.*, *Journal of Environmental Management* (2011) **92** (3), 311
148. Akpan, U., and Hameed, B., *Journal of hazardous materials* (2009) **170** (2), 520
149. Saquib, M*., et al.*, *Desalination* (2008) **219** (1-3), 301
150. Chakrabarti, S., and Dutta, B. K., *Journal of hazardous materials* (2004) **112** (3), 269
151. Liu, S*., et al.*, *Journal of Photochemistry and Photobiology A: Chemistry* (2006) **179** (1), 75
152. Sun, J*., et al.*, *Journal of hazardous materials* (2008) **155** (1), 312
153. Serpone, N*., et al.*, *Journal of photochemistry and photobiology A: Chemistry* (1996) **94** (2-3), 191
154. Grzechulska, J., and Morawski, A. W., *Applied Catalysis B: Environmental* (2002) **36** (1), 45
155. Daneshvar, N*., et al.*, *Journal of Photochemistry and Photobiology A: Chemistry* (2003) **157** (1), 111
156. Huang, M*., et al.*, *Dyes and Pigments* (2008) **77** (2), 327
157. Baran, W*., et al.*, *Dyes and Pigments* (2008) **76** (1), 226
158. Sakthivel, S*., et al.*, *Solar Energy Materials and Solar Cells* (2003) **77** (1), 65
159. WEI, C.-h*., et al.*, *Journal of Environmental Sciences* (2007) **19** (1), 90
160. Sun, M*., et al.*, *Nanotechnology* (2010) **21** (35), 355601
161. Lee, S. W*., et al.*, *Journal of Photochemistry and Photobiology A: Chemistry* (2011) **221** (1), 71
162. Wang, J*., et al.*, *Applied Catalysis B: Environmental* (2013) **136**, 94
163. Kim, D. H*., et al.*, *Journal of Alloys and Compounds* (2004) **375** (1), 259
164. Formo, E*., et al.*, *Nano Letters* (2008) **8** (2), 668
165. Choi, W*., et al.*, *The Journal of Physical Chemistry* (1994) **98** (51), 13669
166. Chen, J*., et al.*, *Applied Catalysis A: General* (2015) **495**, 131
167. Cai, J*., et al.*, *Journal of Materials Chemistry A* (2017) **5** (31), 16412
168. Umebayashi, T*., et al.*, *Journal of Physics and Chemistry of Solids* (2002) **63** (10), 1909
169. Yalçın, Y*., et al.*, *Applied Catalysis B: Environmental* (2010) **99** (3), 469
170. Zhu, J*., et al.*, *Applied Catalysis B: Environmental* (2006) **62** (3-4), 329
171. Yamashita, H*., et al.*, *Journal of synchrotron radiation* (2001) **8** (2), 569
172. Di Paola, A*., et al.*, *The Journal of Physical Chemistry B* (2002) **106** (3), 637
173. Remita, H*., et al.*, *Visible Light-Active Photocatalysis: Nanostructured Catalyst Design, Mechanisms, and Applications* (2018), 129
174. Yao, Y.-C*., et al.*, *Applied Surface Science* (2016) **387**, 469
175. Guo, G*., et al.*, *Talanta* (2009) **79** (3), 570
176. He, X*., et al.*, *Journal of Materials Chemistry* (2011) **21** (2), 475
177. Liu, R*., et al.*, *The Journal of Physical Chemistry C* (2012) **116** (33), 17721
178. Sangpour, P*., et al.*, *The Journal of Physical Chemistry C* (2010) **114** (33), 13955
179. Wang, C. M*., et al.*, *Journal of the American Chemical Society* (1992) **114** (13), 5230
180. Xie, B*., et al.*, *Catalysis Communications* (2005) **6** (11), 699
181. Ye, M*., et al.*, *Journal of the American Chemical Society* (2012) **134** (38), 15720
182. Sakthivel, S*., et al.*, *Water research* (2004) **38** (13), 3001
183. Kim, S*., et al.*, *The Journal of Physical Chemistry B* (2005) **109** (51), 24260
184. Zhang, W*., et al.*, *Catalysis Today* (2004) **93**, 589
185. Li, H*., et al.*, *Journal of the American Chemical Society* (2007) **129** (15), 4538
186. Subramanian, V*., et al.*, *Langmuir* (2003) **19** (2), 469
187. Chen, X., and Burda, C., *Journal of the American Chemical Society* (2008) **130** (15), 5018
188. Ohno, T*., et al.*, *Chemistry Letters* (2003) **32** (4), 364
189. Cong, Y*., et al.*, *The Journal of Physical Chemistry C* (2007) **111** (19), 6976

190. Umebayashi, T*., et al.*, *Chemistry Letters* (2003) **32** (4), 330
191. Choi, Y*., et al.*, *Journal of Materials Science* (2004) **39** (5), 1837
192. Asahi, R*., et al.*, *science* (2001) **293** (5528), 269
193. Wang, Q*., et al.*, *Nanoscale* (2017) **9** (41), 16046
194. Etacheri, V*., et al.*, *ACS applied materials & interfaces* (2013) **5** (5), 1663
195. Dong, H*., et al.*, *Journal of nanoscience and nanotechnology* (2016) **16** (3), 2646
196. Dai, K*., et al.*, *Journal of Nanomaterials* (2014) **2014**, 4
197. Dembele, K. T*., et al.*, *The Journal of Physical Chemistry C* (2013) **117** (28), 14510
198. Ahmmad, B*., et al.*, *Catalysis Communications* (2008) **9** (6), 1410
199. Ou, Y*., et al.*, *Chemical Physics Letters* (2006) **429** (1), 199
200. Natarajan, T. S*., et al.*, *Catalysis today* (2017) **282**, 13
201. Novoselov, K. S*., et al.*, *science* (2004) **306** (5696), 666
202. Ferrari, A. C*., et al.*, *Physical review letters* (2006) **97** (18), 187401
203. Nair, R. R*., et al.*, *Science* (2008) **320** (5881), 1308
204. Zhu, P*., et al.*, *ACS applied materials & interfaces* (2012) **4** (2), 581
205. Yang, M.-Q*., et al.*, *ACS applied materials & interfaces* (2013) **5** (3), 1156
206. Qiu, B*., et al.*, *Journal of the American Chemical Society* (2014) **136** (16), 5852
207. Štengl, V*., et al.*, *Chem. Cent. J* (2013) **7** (1), 41
208. Eid, C*., et al.*, *RSC Advances* (2015) **5** (118), 97849
209. Hummers Jr, W. S., and Offeman, R. E., *Journal of the American Chemical Society* (1958) **80** (6), 1339
210. Lavanya, T*., et al.*, *Journal of Alloys and Compounds* (2014) **615**, 643
211. Zhou, Y*., et al.*, *Chemistry of Materials* (2009) **21** (13), 2950
212. Gómez-Navarro, C*., et al.*, *Nano letters* (2007) **7** (11), 3499
213. Zhu, Y*., et al.*, *Advanced materials* (2010) **22** (35), 3906
214. Huang, Q*., et al.*, *ACS Catalysis* (2013) **3** (7), 1477
215. Bukowski, B., and Deskins, N. A., *Physical Chemistry Chemical Physics* (2015) **17** (44), 29734
216. Lee, J. S*., et al.*, *Advanced Materials* (2012) **24** (8), 1084
217. Kim, I. Y*., et al.*, *Small* (2012) **8** (7), 1038
218. Zhang, H*., et al.*, *ACS nano* (2009) **4** (1), 380
219. Li, Y*., et al.*, *Materials Science in Semiconductor Processing* (2014) **27**, 695
220. Yeh, T.-F*., et al.*, *Materials Today* (2013) **16** (3), 78
221. Wang, X*., et al.*, *New Journal of Chemistry* (2014) **38** (12), 6139
222. Yang, G*., et al.*, *Journal of Materials Chemistry* (2010) **20** (25), 5301
223. Kim, C. H*., et al.*, *Carbon* (2012) **50** (7), 2472
224. Wang, D.-H*., et al.*, *Nanoscale* (2012) **4** (2), 576
225. Cao, S*., et al.*, *Journal of Materials Chemistry* (2011) **21** (47), 19124
226. Ihara, T*., et al.*, *Applied Catalysis B: Environmental* (2003) **42** (4), 403
227. Rengifo-Herrera, J*., et al.*, *Applied Catalysis B: Environmental* (2009) **88** (3), 398
228. Dong, F*., et al.*, *Nanotechnology* (2008) **19** (36), 365607
229. Cheng, X*., et al.*, *Arabian Journal of Chemistry* (2016) **9**, S1706
230. Wang, H*., et al.*, *Chemical Society Reviews* (2014) **43** (15), 5234
231. Robert, D., *Catalysis Today* (2007) **122** (1), 20
232. Kuang, S*., et al.*, *Applied Surface Science* (2009) **255** (16), 7385
233. Ren, G*., et al.*, *J. Chem. Soc. Pak* (2011) **33** (5), 666
234. Shang, J*., et al.*, *Applied Catalysis A: General* (2004) **257** (1), 25
235. Sun, S*., et al.*, (2000)
236. Ouyang, J*., et al.*, *Journal of Materials Science* (2012) **47** (9), 4187
237. Zhang, H*., et al.*, *Journal of Materials Chemistry* (2009) **19** (29), 5089
238. Liqiang, J*., et al.*, *Solar Energy Materials and Solar Cells* (2006) **90** (12), 1773
239. Li, G.-S*., et al.*, *Environmental science & technology* (2009) **43** (18), 7079

240. Khan, H.*, et al.*, *Applied Catalysis B: Environmental* (2018) **226**, 311
241. Daghrir, R.*, et al.*, *Industrial & Engineering Chemistry Research* (2013) **52** (10), 3581
242. Zhou, H.*, et al.*, *Energy & Environmental Science* (2012) **5** (5), 6732
243. Yang, Z.*, et al.*, *Chemical reviews* (2011) **111** (5), 3577
244. Wang, M.*, et al.*, *Small* (2015) **11** (12), 1436
245. Wang, M.*, et al.*, *Energy & Environmental Science* (2013) **6** (4), 1211
246. Park, H.*, et al.*, *Journal of Materials Chemistry* (2008) **18** (20), 2379
247. Tada, H.*, et al.*, *Nature materials* (2006) **5** (10), 782
248. Hao, R.*, et al.*, *Applied Catalysis B: Environmental* (2016) **187**, 47
249. Dinh, C. T.*, et al.*, *Angewandte Chemie International Edition* (2014) **53** (26), 6618
250. Chen, Y.*, et al.*, *ACS applied materials & interfaces* (2014) **6** (16), 14405
251. Jiang, T.*, et al.*, *Nanoscale* (2015) **7** (1), 209
252. Kang, Q.*, et al.*, *Angewandte Chemie* (2015) **127** (3), 855
253. Park, H.*, et al.*, *The Journal of Physical Chemistry C* (2011) **115** (13), 6141
254. Xu, J.-W.*, et al.*, *ACS applied materials & interfaces* (2014) **6** (17), 15122
255. Marchal, C.*, et al.*, *Advanced Energy Materials* (2018)
256. Kabra, K.*, et al.*, *Industrial & engineering chemistry research* (2004) **43** (24), 7683
257. Doh, S. J.*, et al.*, *Journal of Hazardous Materials* (2008) **154** (1), 118
258. Du, P.*, et al.*, *Journal of Materials Science* (2013) **48** (24), 8386
259. Jeswani, H. K.*, et al.*, *Journal of Cleaner Production* (2015) **89**, 203
260. Noziere, B.*, et al.*, *Chemical reviews* (2015) **115** (10), 3919
261. Schaider, L. A.*, et al.*, *Science of the Total Environment* (2014) **468**, 384
262. Yan, Z.*, et al.*, *International Journal of Photoenergy* (2014) **2014**
263. Quero-Pastor, M.*, et al.*, *Journal of environmental management* (2014) **137**, 197
264. Straaten, N.*, et al.*, Degradation of hydrocarbons under methanogenic conditions in different geosystems. In *EGU General Assembly Conference Abstracts*, (2014), Vol. 16, p 6151
265. von der Ohe, P. C., and Goedkoop, W., *Science of the Total Environment* (2013) **444**, 480
266. Van der Bruggen, B., and Vandecasteele, C., *Environmental pollution* (2003) **122** (3), 435
267. Tahir, K.*, et al.*, *Journal of Photochemistry and Photobiology B: Biology* (2016) **162**, 189
268. Dong, S.*, et al.*, *Journal of Chemical Technology and Biotechnology* (2015) **90** (5), 880
269. Kavitha, V.*, et al.*, *International Journal of Nanoscience* (2016) **15** (05n06), 1660002
270. Prabhu, S.*, et al.*, *Indian Journal of Materials Science* (2014) **2014**
271. He, M.*, et al.*, *Express Polymer Letters* (2014) **8** (11)
272. Jain, A. K.*, et al.*, *Octa Journal of Environmental Research* (2015) **3** (1)
273. Sood, S.*, et al.*, *Ceramics International* (2015) **41** (3), 3533
274. Zhang, D.*, et al.*, *Kinetics and Catalysis* (2015) **56** (5), 569
275. Niu, Y.*, et al.*, *Catalysis Today* (2013) **201**, 159
276. Sabar, S.*, et al.*, *Desalination and Water Treatment* (2016) **57** (13), 5851
277. Akpan, U., and Hameed, B., *Desalination and Water Treatment* (2014) **52** (28-30), 5639
278. Wang, P.*, et al.*, *Water research* (2011) **45** (16), 5015
279. Senthilnathan, J., and Philip, L., *Chemical engineering journal* (2010) **161** (1), 83
280. de Vries, W.*, et al.*, Critical loads of heavy metals for soils. In *Heavy metals in soils*, Springer(2013), pp 211
281. Wong, Y. E., (2015)
282. Bolan, N.*, et al.*, *Journal of Hazardous Materials* (2014) **266**, 141
283. Schrank, S.*, et al.*, *Journal of photochemistry and photobiology A: Chemistry* (2002) **147** (1), 71
284. Sreekantan, S.*, et al.*, *The European Physical Journal Applied Physics* (2014) **67** (1), 10404
285. Zhang, F.-S.*, et al.*, *Journal of Photochemistry and Photobiology A: Chemistry* (2004) **167** (2), 223
286. Keane, D. A.*, et al.*, *Catalysis Science & Technology* (2014) **4** (5), 1211

287. Matsunaga, T*., et al.*, *FEMS Microbiology letters* (1985) **29** (1-2), 211
288. Lee, O.-M*., et al.*, *Journal of hazardous materials* (2015) **295**, 201
289. Matsunaga, T*., et al.*, *Applied and environmental microbiology* (1988) **54** (6), 1330
290. Huang, Z*., et al.*, *Journal of Photochemistry and photobiology A: Chemistry* (2000) **130** (2), 163
291. Nadtochenko, V*., et al.*, *Journal of Photochemistry and Photobiology A: Chemistry* (2006) **181** (2), 401
292. Maness, P.-C*., et al.*, *Applied and environmental microbiology* (1999) **65** (9), 4094
293. Kiwi, J., and Nadtochenko, V., *The Journal of Physical Chemistry B* (2004) **108** (45), 17675
294. Suwalsky, M*., et al.*, *Journal of Photochemistry and Photobiology B: Biology* (2005) **78** (3), 253
295. Rakovich, Y. P., *KnE Energy & Physics* (2018) **3** (2), 416
296. Bauman, T. M*., et al.*, *BMJ case reports* (2018) **2018**, bcr
297. Garg, A. D*., et al.*, *Cancer Immunology, Immunotherapy* (2018), 1
298. Shang, H*., et al.*, *Journal of Photochemistry and Photobiology B: Biology* (2017) **177**, 112
299. Pinaud, B. A*., et al.*, *Energy & Environmental Science* (2013) **6** (7), 1983
300. Nishimoto, S.-i*., et al.*, *Journal of the Chemical Society, Faraday Transactions 1: Physical Chemistry in Condensed Phases* (1985) **81** (10), 2467
301. Higashimoto, S*., et al.*, *Catalysis Science & Technology* (2013) **3** (2), 400
302. Ni, M*., et al.*, *Renewable and Sustainable Energy Reviews* (2007) **11** (3), 401
303. Hisatomi, T*., et al.*, *Chemical Society Reviews* (2014) **43** (22), 7520
304. Liu, E*., et al.*, *Nanotechnology* (2014) **25** (16), 165401
305. Wang, Q*., et al.*, *Chemistry of Materials* (2014) **26** (14), 4144
306. Hagiwara, H*., et al.*, *Catalysts* (2016) **6** (3), 42
307. Xu, D*., et al.*, *Langmuir* (2015) **31** (35), 9694
308. Xu, J., and Cao, X., *Chemical Engineering Journal* (2015) **260**, 642
309. Wang, H*., et al.*, *International Journal of Hydrogen Energy* (2015) **40** (1), 340
310. Puskelova, J*., et al.*, *Applied Surface Science* (2014) **305**, 665
311. Nomikos, G. N*., et al.*, *Applied Catalysis B: Environmental* (2014) **146**, 249
312. Haryanto, A*., et al.*, *Energy & Fuels* (2005) **19** (5), 2098
313. Kennedy, J*., et al.*, *Catalysis, Structure & Reactivity* (2015) **1** (1), 35
314. DuChene, J. S*., et al.*, *Nano letters* (2018) **18** (4), 2545
315. Landers, A. T*., et al.*, *ACS Energy Letters* (2018) **3**, 1450
316. Ran, J*., et al.*, *Advanced materials* (2018) **30** (7), 1704649
317. Lei, Z*., et al.*, *Catalysis Communications* (2018) **108**, 27
318. Jiang, Z*., et al.*, *Chemical Engineering Journal* (2018) **348**, 592
319. Eranna, G., *Metal oxide nanostructures as gas sensing devices*. CRC Press: 2016
320. Park, J. Y*., et al.*, *Nanotechnology* (2017) **28** (9), 095502
321. Wu, P*., et al.*, *Nanotechnology* (2018) **29** (18), 184005
322. Zou, Z*., et al.*, *Journal of Alloys and Compounds* (2015) **645**, 17
323. Zhang, J*., et al.*, *Journal of Nanoscience and Nanotechnology* (2018) **18** (5), 3185
324. Li, G*., et al.*, *Water research* (2015) **86**, 17
325. Wang, Q*., et al.*, *Journal of hazardous materials* (2016) **307**, 213
326. Zhu, Z*., et al.*, *Ceramics International* (2016) **42** (6), 6749
327. Karaolia, P*., et al.*, *Applied Catalysis B: Environmental* (2018) **224**, 810
328. Han, E*., et al.*, *Energy & Fuels* (2018) **32** (4), 4357
329. Nada, A. A*., et al.*, *The Journal of Physical Chemistry C* (2017) **121** (44), 24669
330. Vaiano, V*., et al.*, *Applied Catalysis B: Environmental* (2015) **170**, 153
331. Tahir, M*., et al.*, *Journal of CO2 Utilization* (2017) **18**, 250
332. Dong, W*., et al.*, *Applied Surface Science* (2015) **349**, 279
333. Khanchandani, S*., et al.*, *ACS Sustainable Chemistry & Engineering* (2016) **4** (3), 1487

334. Zubair, M.*, et al.*, *Journal of CO2 Utilization* (2018) **26**, 70
335. Kemell, M.*, et al.*, *Chemistry of Materials* (2007) **19** (7), 1816
336. Abdel-Maksoud, Y.*, et al.*, *Catalysts* (2016) **6** (9), 138
337. Blanco J., M. S., *UNESCO Org. Pub., Paris* (2003)
338. Poux, M.*, et al.*, *Green process engineering: From concepts to industrial applications*. CRC Press: 2015
339. Hendarsa, A. S., and , H. H., Slamet *International Journal of Engineering & Technology* (2013) **13**